A Glycymeris-rich unit as evidence of a late Pleistocene tsunami event from NW Algeria: A biostratigraphic, taphonomic, and sedimentological approach

Mohamed Amine Doukani, Linda Satour, Caner Kaya Ozer, Lahcene Belkebir, Antje H.L. Voelker, Hassane Tedjeddine, Bernard Landau, Alfred Uchman, Mostefa Bessedik, Markes E. Johnson, Ana Hipólito, José Madeira, Sérgio P. Ávila

Quaternary Science Reviews 368 (2025) 109552

Contents lists available at ScienceDirect

Quaternary Science Reviews

journal homepage: www.elsevier.com/locate/quascirev

A *Glycymeris*-rich unit as evidence of a late Pleistocene tsunami event from NW Algeria: A biostratigraphic, taphonomic, and sedimentological approach

Mohamed Amine Doukani [a,*], Linda Satour [a], Caner Kaya Ozer [b], Lahcene Belkebir [a], Antje H.L. Voelker [c,d], Hassane Tedjeddine [a], Bernard Landau [e,f,g], Alfred Uchman [h], Mostefa Bessedik [a], Markes E. Johnson [i], Ana Hipólito [j,k], José Madeira [g], Sérgio P. Ávila [j,k,l,m]

[a] *Laboratoire de Paléontologie Stratigraphique et Paléoenvironnement, FSTU, University of Oran 2 Mohamed Ben Ahmed, BP.1524 El M'Naouer, 31000, Oran, Algeria*
[b] *Department of Geological Engineering, Engineering and Architecture Faculty, Yozgat Bozok University, Yozgat, Turkey*
[c] *Divisão de Geologia e Georecursos Marinhos, Instituto Português do Mar e da Atmosfera (IPMA), Avenida Doutor Alfredo Magalhães Ramalho 6, 1495-165, Algés, Portugal*
[d] *Centro de Ciências do Mar do Algarve (CCMAR/CIMAR LA), Campus de Gambelas, Universidade do Algarve, 8005-139, Faro, Portugal*
[e] *Naturalis Biodiversity Center, P.O. Box 9517, 2300, RA Leiden, the Netherlands*
[f] *International Health Centres, Av. Infante de Henrique 7, Areias São João, P-8200 Albufeira, Portugal*
[g] *Instituto Dom Luiz, Faculdade de Ciências, Universidade de Lisboa, Campo Grande, 1749-016 Lisboa, Portugal*
[h] *Faculty of Geography and Geology, Institute of Geological Sciences, Jagiellonian University, Gronostajowa 3a, Kraków, PL 30-387, Poland*
[i] *Department of Geosciences, Williams College, Williamstown, MA, 01267, USA*
[j] *CIBIO, Centro de Investigação em Biodiversidade e Recursos Genéticos, InBIO Laboratório Associado, Pólo dos Açores, BIOPOLIS Program in Genomics, Biodiversity and Land Planning, Portugal*
[k] *MPB-Marine Palaeontology and Biogeography laboratory, University of the Azores, Rua da Mãe de Deus, 9501-801, Portugal*
[l] *Departamento de Biologia, Universidade dos Açores, 9501-801, Ponta Delgada, Açores, Portugal*
[m] *UNESCO Chair – Land Within Sea: Biodiversity & Sustainability in Atlantic Islands, University of the Azores, Rua da Mãe de Deus, 9500-321, Ponta Delgada, Portugal*

ARTICLE INFO

Handling Editor. Biagio Giaccio

Keywords:
Glycymeris
Taphonomy
Quaternary
Last interglacial
Tsunami deposit
Senegalese fauna
Western mediterranean
Algeria

ABSTRACT

Compared to the extensive research carried out on the Neogene deposits of the Lower Chelif Basin, the Pleistocene series is still poorly studied, with no detailed lithological succession published to date. This study focuses on the *Glycymeris*-rich Unit (GRU) along the coastal area of the Hachacha Plateau in Northwestern Algeria. This unit unconformably overlies Miocene, Pliocene, and Pleistocene basements. The latter was identified for the first time in this work using a biostratigraphic approach based on calcareous nannofossils and planktonic foraminifera. The GRU is interpreted as a tsunami-related deposit, formed in a coastal environment (foreshore/backshore) during the upper Pleistocene, corresponding to the Last Interglacial period, i.e., Marine Isotopic Substage 5e (MIS 5e). This interpretation provides a first multidisciplinary description of a tsunami deposit in Algeria that is supported by distinctive biotic, taphonomic, and sedimentological features. The deposits contain a mixture of marine organisms from different ecological zones (supralittoral to shallow circalittoral biocenoses), including molluscan assemblages such as the so-called Senegalese fauna (bivalves and gastropods), sponges, serpulids, coralline algae and corals. Occasionally, rare terrestrial snails are also found mixed with the marine fauna. Taphonomic analysis reveals low percentages of boring, absence of encrustation, and excellent shell preservation, suggesting that powerful waves eroded sediment masses and transported them inland from deeper areas beneath the taphonomic active zone. The predominance of sharp-edged fragmented shells, chaotic arrangements with oblique to vertical shell orientations and the good shell sorting, indicates transport by mass flows and rapid deposition during an extreme event – a tsunami –, distinguishing these deposits from those associated with gradual and oscillatory flows, such as storm events. Sedimentological characteristics, including irregular erosive base, lateral facies variations, wide grain size ranges (clay to boulders), normal and inverse grading, and diagnostic structures (both fragile and hard-rock rip-up clasts, high-energy flow features such as horizontal and oblique laminations, and hummocky cross-stratification, injection of sediment into the substrate, imbrication of

* Corresponding author.
E-mail addresses: doukanimohamedamine@gmail.com, doukani.mohamed@univ-oran2.dz (M.A. Doukani).

https://doi.org/10.1016/j.quascirev.2025.109552
Received 15 January 2025; Received in revised form 24 July 2025; Accepted 28 July 2025
Available online 6 August 2025

large angular boulders and soft sediment deformation structures), combined with the active tectonic context of Northwestern Algeria support the interpretation as a seismically triggered tsunami and enhances the understanding of this type of deposits in similar coastal settings.

1. Introduction

Shell beds are classified genetically into three categories in a triangular diagram (Kidwell et al., 1986): biogenic, diagenetic and sedimentological concentrations. The latter are the result of physical processes, with the dominance of allochthonous shells. This type of accumulation is the most common in coastal areas and is often linked to high-energy hydraulic events, such as storms or tsunamis (Gutiérrez-Mas et al., 2009; Massari et al., 2009; Reinhardt et al., 2012; Ávila et al., 2015b; Benyoucef et al., 2021; Torres et al., 2022).

During the last three decades, numerous studies have synthesized the Quaternary deposits around the Western Mediterranean region (Zazo, 1999; Mauz and Hassler, 2000; Zazo et al., 2003, 2013; Bardaji et al., 2009; Mauz et al., 2009; Torres et al., 2010, 2015; Andreucci et al., 2014; Cerrone et al., 2021; Del Valle et al., 2024). However, references to the marine Pleistocene of Northern Algeria remain scarce, with but a few studies focusing on the Quaternary evolution in the context of neotectonic activity and palaeoseismological evidence (Meghraoui et al., 1996; Abbouda et al., 2019; Maouche et al., 2019; Guessoum et al., 2018).

In Algeria, the upper Pleistocene marine series was studied for the first time by De Lamothe (1911), followed by other works by Doumergue (1922), Anderson (1936), Dalloni (1953), Gourinard (1958), and Thomas (1985). It is the result of a transgressive phase, generally represented by coastal deposits, which are highly fossiliferous with a notable abundance of bivalves and gastropods, forming shell beds – the *Glycymeris*-rich Unit (GRU). Despite the more recent Thomas (1985) study, there still exists a knowledge gap on the last interglacial deposits, in particular those of the warmest period, usually referred to as the Marine Isotopic Substage 5e (MIS 5e). In fact, when compared to the numerous studies on the Neogene series of the Lower Chelif Basin (Algeria), including those on biostratigraphy (Perrodon, 1957; Mazzola, 1971; Belkebir and Anglada, 1985; Belkebir et al., 1996, 2008; Bessedik et al., 2002; Atif et al., 2008; Belhadji et al., 2008; Mansouri et al., 2008; Osman et al., 2021; Atik et al., 2024), geodynamic and palaeogeographic evolution (Anderson, 1936; Delteil, 1974; Meghraoui, 1982; Thomas, 1985; Neurdin-Trescartes, 1992, 1995; Badji et al. 2015; Arab et al., 2015; Leprêtre et al., 2018), as well as other works on the systematics and evolution of their fossil content, in particular the molluscs (Freneix et al., 1987a, b, 1988; Satour et al., 2011, 2013, 2020; Benyoucef et al., 2021; Benyoucef and Landau, 2025), the Pleistocene series remains poorly studied and, to date, no detailed lithologic succession has been published.

In the present study, we focus on Pleistocene outcrops located along the coast of the Hachacha Plateau, in Northwestern Algeria. This research represents the first detailed lithostratigraphic study of the Pleistocene in the region, with particular emphasis on calcareous nannofossils and planktonic foraminifera to establish the age of the lenticular marl outcrops in the Port de Ménard and Sedaoua sectors. Additionally, a GRU dating approach is attempted based on the mollusc assemblage associations. Our comprehensive approach integrates sedimentological and taphonomic analyses to better understand the evolution of the Hachacha Plateau coastline during the Last Interglacial period, and to constrain the depositional environments and the processes responsible for the formation of the GRU. Within this framework, we aim to distinguish between two possible large-scale events (tsunami or storm), thus enabling comparisons with other extreme events documented across the Phanerozoic, as well as provide a tectonic context, to elucidate the history of this coastal region during the Last Interglacial period, i.e., Marine Isotopic Substage 5e (MIS 5e).

1.1. Tsunamites versus tempestites: how to distinguish them?

The differentiation between deposits associated with tsunamis (tsunamites) and those resulting from storms (tempestites) remains a challenge, given that the criteria for distinguishing them from other marine sedimentary deposits are mostly identical. Recently, and following the 2004 Indian Ocean tsunami, there has been a surge of interest among researchers in catastrophic processes and tsunami deposits, with a particular focus on their comparison to those linked to storms (Goff et al., 2004; Puga-Bernabéu and Aguirre, 2017; Khadraoui et al., 2018; Paris et al., 2018; Madeira et al., 2020; Sztanó et al., 2020; Ramírez-Herrera et al., 2012; Torres et al., 2022; Ávila et al., 2025).

Previously, any sedimentological concentration of shells deposited in a shallow environment or the coastal area was thought to be a storm deposit, based on many sedimentological and taphonomic characteristics such as size grading, shell stacking, shell sorting, shell fragmentation, concavity orientation, and basal and upper contact type (Aigner, 1985; Kidwell et al., 1986; Kidwell and Holland, 1991; Seilacher and Aigner, 1991). More recently, the skeletal concentrations produced by up-rush flow (landwards) or backwash flows (basinwards) have been interpreted as the result of high-energy hydraulic events (e.g., storms, hurricanes, and tsunamis; Puga-Bernabéu and Aguirre, 2017). From a palaeontological point of view, several taphonomic criteria identify the skeletal concentrations produced by a tsunamigenic event. These include: i) a mixture of organisms from different environments, including terrestrial as well as marine organisms (e.g., pelagic, shallow-water, deep-water) (Paris et al., 2018); ii) out of life positions with the dominance of angular fragmentation (Dawson and Stewart, 2007; Donato et al., 2008); iii) shells may display a variety of settling position, ranging from chaotic to normal (Massari et al., 2009; Engel et al., 2016), or reverse grading (Massari et al., 2009); iv) standardized 1-kg of fossiliferous sediments collected from tsunami deposits usually yield higher values of richness and evenness in comparison with samples from storm deposits (Ávila et al., 2025); and v) the proportion of large, heavy shells in the molluscan assemblages in palaeotsunami deposits is a valid index of tsunami strength on coastal lowlands inside shallow coral reef lagoons (Kitamura et al., 2018). Tsunami-related marine shell deposits are typically characterized by denser, thicker, and more extensive beds, with shells exhibiting good to excellent preservation and a predominance of shells oriented obliquely to perpendicularly to the base of the deposit, often dominated by a single species (Puga-Bernabéu and Aguirre, 2017). These features have been confirmed by Torres et al. (2022), who interpreted mollusc shell accumulations from the Torrevieja-La Mata coast (Southeastern Spain) as the result of tsunami events during the late Pleistocene.

Based on Holocene tsunami deposits from Eastern Japan, Fujiwara and Kamataki (2007) proposed a tsunami facies model consisting of four vertical units, Tna to Tnd in ascending order, reflecting the temporal variation of wave sizes within tsunami wave trains. Shanmugam (2012) concluded that the hummocky cross-stratification (HCS) and traction carpet that characterize the Tnb unit of Fujiwara and Kamataki (2007) cannot be produced by a single depositional event, thus rejecting tsunami as the promoter agent, because it is hydrodynamically untenable. For Morton et al. (2007), if there is a source of fine terrigenous sediments, rip-up clasts and internal mud layers will be a diagnostic criterion to distinguish between tsunamites (that hold those features) and storm deposits (where fine terrigenous sediments are absent). Among the hydrodynamic criteria for tsunamis are a large wavelength, longer wave period, uniform distribution of kinetic energy in the water column and a fewer number of waves. These characteristics allow the

inland transport of large boulders or rip-up clasts from the underlying cohesive substrate, as well as masses of suspended sediment (Engel and Brückner, 2011; Shanmugam, 2012; Engel et al., 2016; Marriner et al., 2017).

2. Geological context and tectonics

The Hachacha Plateau lies Northwest of the Dahra Massif (Fig. 1). The latter is formed by several allochthonous units from the Cretaceous to the Paleogene, separating the Neogene and the Quaternary terrains of the Lower Chelif Basin to the South from those to the North (Delteil, 1974). This region is represented by a succession of Miocene, Pliocene, and Quaternary deposits overlying the Mesozoic and Paleogene basement (Perrodon, 1957; Arab et al., 2015), with traces of Alpine tectonics still active today (Guardia, 1975; Ouyed et al., 1981; Meghraoui, 1982; Meghraoui et al., 1996; Matougui and Haddoum, 2008; Badji et al., 2015; Leprêtre et al., 2018; Abbouda et al., 2019). This succession is characterized by a sedimentary fill that can be divided into three distinct megasequences (Delfaud et al., 1973; Thomas, 1985; Neurdin-Trescartes, 1992). Megasequences I and II represent the Miocene marine deposits formed during the first and second post-nappe cycles (Perrodon, 1957; Meghraoui, 1982; Meghraoui et al., 1988). The first magasequence (late Burdigalian-Serravallian; Belkebir and Anglada, 1985; Belkebir et al., 1996; Bessedik et al., 2002; Belkebir et al., 2008) was deposited above the active Tellian allochthon during a compression episode, forming a foreland basin (Arab et al., 2015). The second megasequence (Tortonian–Messinian) formed during transtensional activity in a thrust-top pull-apart basin (Roure et al., 2012; Arab et al., 2015). The third megasequence extends from the Pliocene to the Pleistocene (Thomas, 1985; Neurdin-Trescartes, 1992) and was deposited during the last compressional episode, parallel to the inversion of the Lower Chelif Basin boundary faults (Arab et al., 2015). The first phase of this megasequence corresponds to a Pliocene transgressive cycle that becomes regressive (Perrodon, 1957; Mazzola, 1971; Belkebir and Anglada, 1985; Rouchy et al., 2007; Atif et al., 2008; Mansouri et al., 2008; Osman et al., 2021; Atik et al., 2024). In the Hachacha Plateau, this cycle is terminated by a thick sandy formation which is marked by the first appearance of the foraminifera *Globoconella inflata* (d'Orbigny, 1839) [= *Globorotalia inflata* (d'Orbigny, 1839; Belkebir and Anglada, 1985). According to Lirer et al. (2019), the first appearance of *G. inflata*, represents in the Mediterranean region the MPI6 zone, which characterizes the lowest stage of the Pleistocene series/epoch (Gelasian). The second phase of the third megasequence is generally represented by continental deposits (Bel Hasel Formation) that evolve laterally into marine facies (Arzew Formation), which locally unconformably overlies the deposits of the first cycle (Thomas, 1985).

Deposits of Calabrian age were identified on the coast of Western Algeria for the first time by Laffitte (1950). In the Hachacha Plateau, these deposits are tilted towards the sea and cover a large area, from Kramis Wadi in the East to Chelif Wadi in the West (Fig. 1). These sediments are discordant on all previous formations and are represented by a shelly conglomerate topped by shelly sandstone and thick aeolian deposits, then crowned by red continental deposits (Laffitte, 1950; Perrodon, 1957) (Fig. 1). The Quaternary along the Algerian coast, from the Sahel of Algiers in the East to Oran in the West, across the Hachacha Plateau, is represented by marine sedimentary deposits arranged in a staircase sequence of marine terraces, thus reflecting local and regional uplifts (De Lamothe, 1911; Glangeaud, 1932; Anderson, 1936; Gourinard, 1958; Thomas, 1985). These uplifts are related to NW-SE shortening, estimated at 5 mm/year, resulting from the convergence of the African and Eurasian plates (DeMets et al., 1990, 2010; Nocquet and Calais, 2004; Billi et al., 2023). The staircase of marine terraces present along the coast represent older shorelines (Gourinard, 1958), and are classified according to their altitude, from the oldest to the recent: (a) the 170-m terrace, (b) the 80-m terrace, (c) the 50-m terrace, (d) the 35-m terrace, and (e) the 15-m terrace (Anderson, 1936). The latter terrace is the subject of this study, and occurs in Northwestern Algeria. Several authors (e.g., De Lamouth, 1911; Doumergue, 1922; Anderson, 1936; Dalloni, 1953; Gourinard, 1958; Thomas, 1985) attributed a Tyrrhenian age (now the upper Pleistocene) to these fossiliferous deposits, based on the presence of *Strombus bubonius* Lamarck, 1822 [now Thetystrombus latus (Gmelin, 1791)] and *Conus testudinarius* Hwass, 1792 (currently a synonym of *Conus ermineus* Born, 1778). At the base of this marine terrace, seismic activity indicators are often found, attesting to the occurrence of earthquakes of magnitude $M > 5.5$ (Guessoum et al., 2018).

Seismic reflection data across the margin offshore the Mostaganem region (Domzig et al., 2006; Badji et al., 2015; Soto et al., 2022), reveal a seismostratigraphic succession starting with pre-salt Miocene deposits set directly on oceanic basement, surmounted by an evaporitic series represented by a mobile unit (MU), and an upper unit (UU) that intersects the Pliocene and Quaternary deposits, which are folded and faulted (Fig. 2). The thickness of these deposits is laterally variable as it is strongly affected by diapiric deformation (Lofi et al., 2011). These diapirs are sealed by upper Quaternary deposits and testify to a salt tectonic phase from the Pliocene to the mid-Quaternary, except for the Ameur diapir that affects the sea floor and crosses the upper Quaternary deposits, allowing authors to postulate that it was probably active until recently (Badji et al., 2015; Soto et al., 2022) (Fig. 2). The recent tectonic activity has reactivated conjugated faults in the Northwestern margin of the Dahra Massif. These faults are responsible for destabilizing the surface cover, which is often affected by various types of landslides (Matougui and Haddoum, 2008) (Fig. 1).

3. Materials and methods

Field campaigns conducted between 2021 and 2024, studied five sections of the Pleistocene series of the Hachacha Plateau coastline, from East to West: Port de Menard, Sid El Adjel, Ain Brahim, Sedaoua, and Kef Boughetar (Figs. 1 and 3). These sections were described and measured, considering the underlying and the overlying deposits, lateral facies variation, geometry, sedimentary structures (Figs. 3 and 4), and fossil content.

The two outcrops representing the Eastern and Western extremities, Port de Menard and Kef Boughetar, were chosen for taphonomic analysis based on the excellent quality of shell preservation, thickness of the sedimentary sequence, and accessibility, to extract the maximum amount of data and ensure meaningful results. This taphonomic analysis was performed following a quantitative approach, according to the methodology described by Yesares-García and Aguirre (2004). Thirteen 1 m-wide squares were used per site, seven at Port de Menard and six at Kef Boughetar to quantify several taphonomic criteria on the abundant *Glycymeris* and *Cardium* bivalve shells, which are perfectly preserved and constitute the main part of the studied unit (GRU). The taphonomic criteria used were the relative abundance of the biotic components per surface, size sorting, percentage of fragmentation, disarticulation, encrustation and bioerosion, concavity orientation, shell angle with the base (concordant, oblique, perpendicular, as proposed by Kidwell et al., 1986) and abrasion (edge roundness-sharpness).

To group the taphonomic results obtained in the different surfaces into distinct classes and evaluate their similarities, we applied a Q-mode cluster analysis. This method focuses on clustering objects (in this case, the taphonomic criteria measured per surface) based on their similarity profiles across measured features. The analysis was conducted using Euclidean distances as the metric for calculating dissimilarities between the surfaces. The clustering process employed the Unweighted Pair Group Method with Arithmetic Mean (UPGMA), a hierarchical clustering technique that iteratively merges groups of surfaces based on their average similarity. This approach enabled us to generate a dendrogram, visually representing the relationships between the surfaces and the formation of clusters at various similarity thresholds. The analysis was performed using PAST v. 4.03 software, ensuring

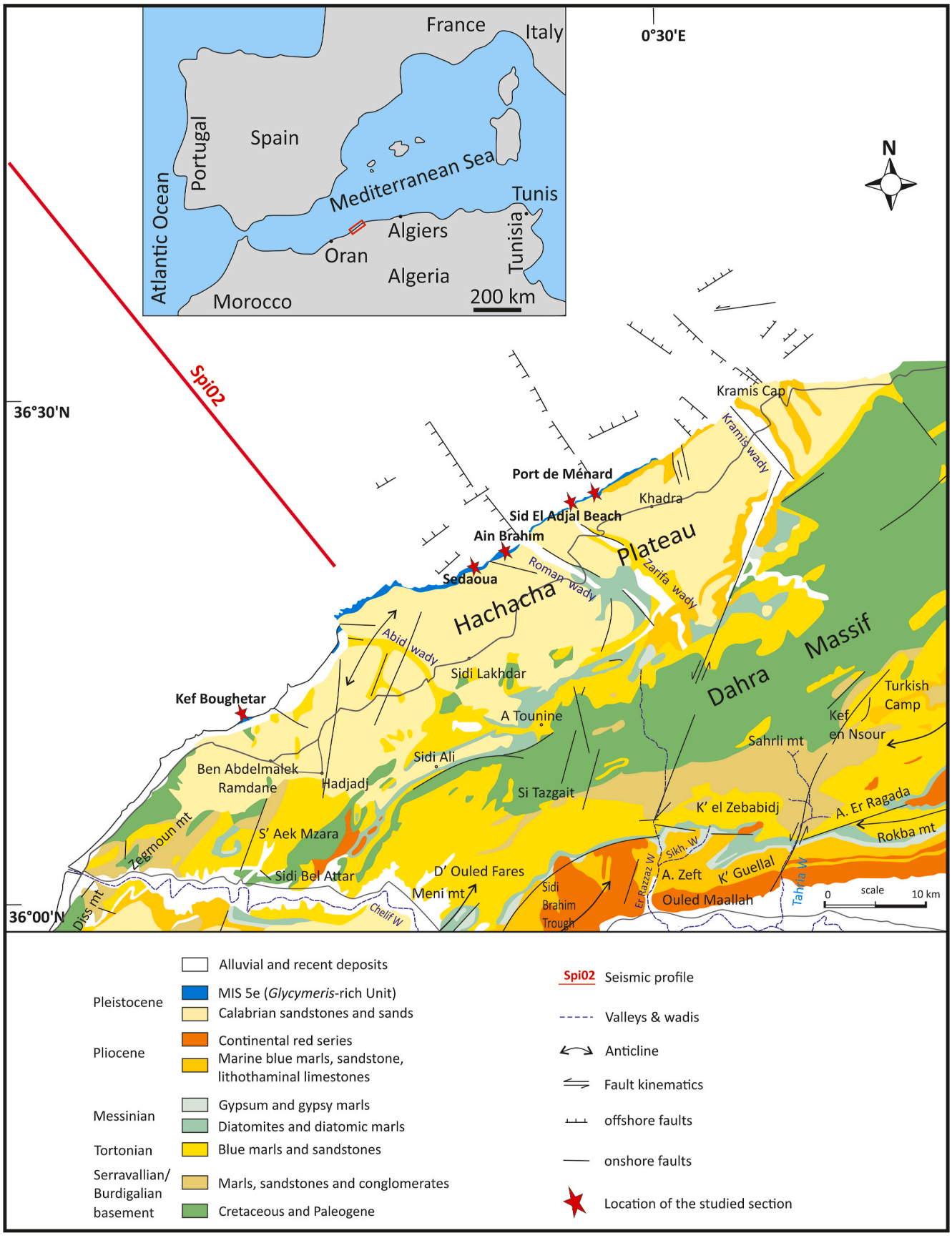

Fig. 1. Geological and structural map of Dahra Massif, and structural context of the Western Dahra margin (modified from: Perrodon, 1957; Meghraoui et al., 1988; Belkebir et al., 2002; Bessedik et al., 2002; Matougui and Haddoum, 2008; Osman et al., 2021).

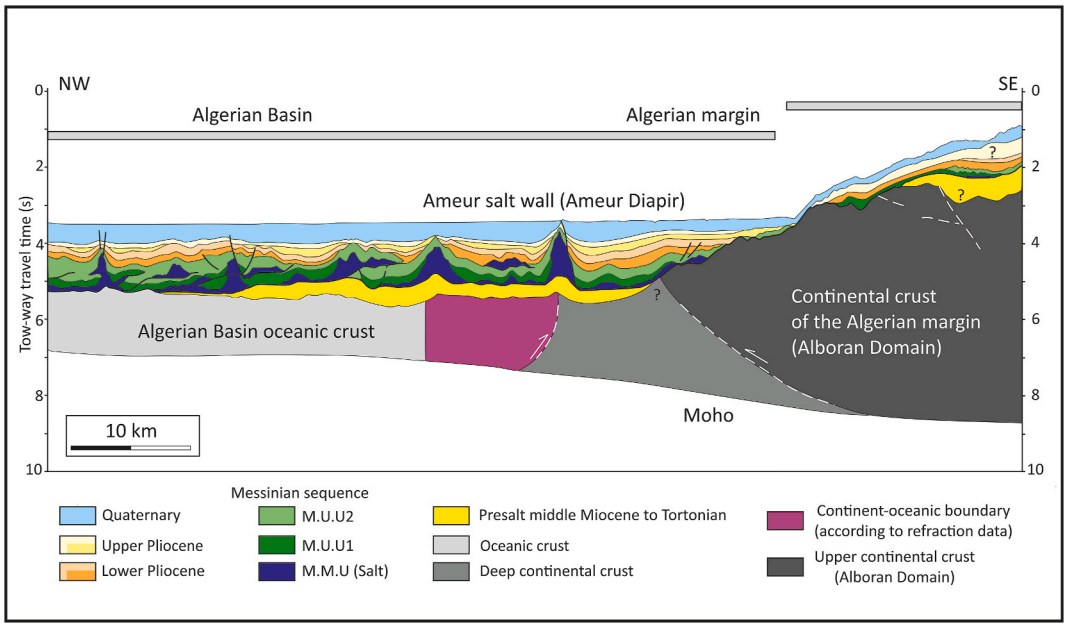

Fig. 2. Interpretation of the seismic line (SPI-O2 profile) from Badji et al. (2015) and detailed in Soto et al. (2022), showing the structure and structural units in the Algerian margin offshore Mostaganem.

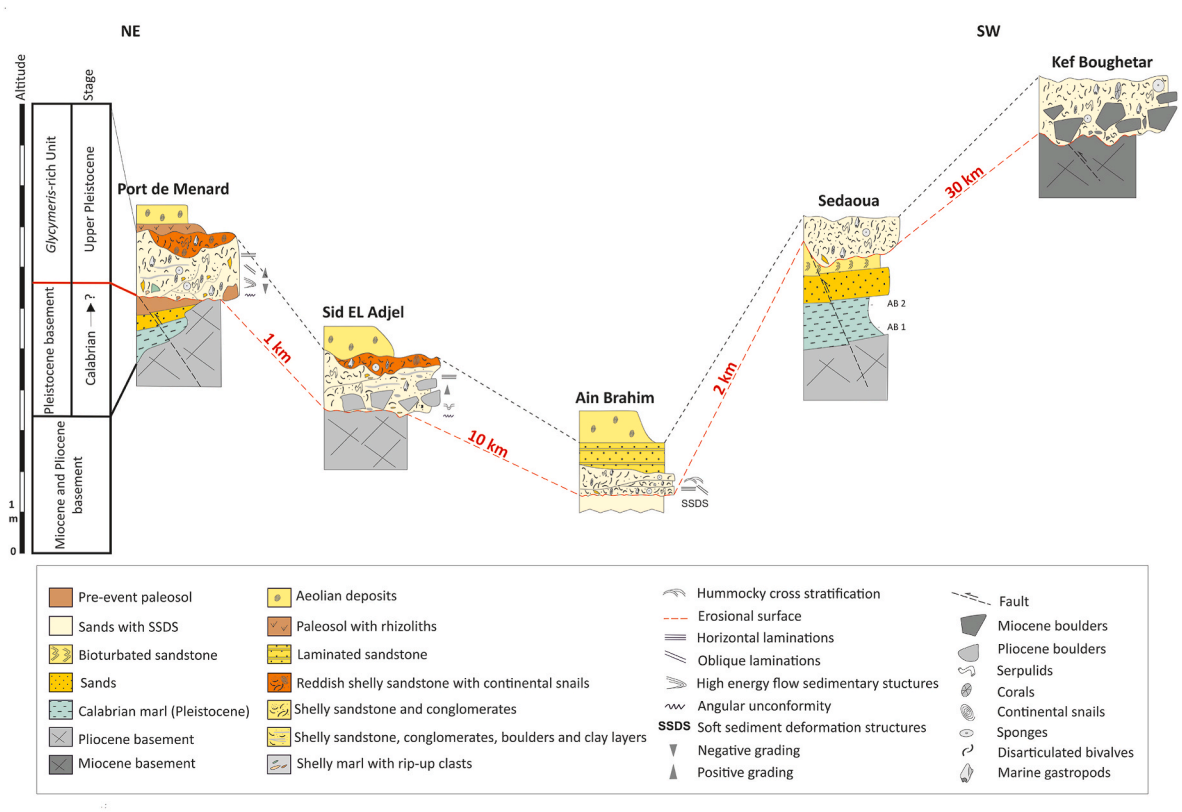

Fig. 3. Correlation of *Glycymeris*-rich unit (GRU) with Senegalese fauna along the sections of Port de Menard, Sid El Adjel, Ain Brahim, Sedaoua and Kef Boughetar. The stratigraphic columns take into account the altitude of the base of the outcrops. The metric scale represents elevation above present sea-level.

reproducibility and accuracy in grouping the results.

3.1. Biostratigraphic dating

Four samples were collected from a lenticular marl layer representing the Pleistocene basement of the study unit (GRU) cropping out at the Port de Menard and Sedaoua sectors, with two samples per section (PM1, PM2 from Port de Menard and AB1, AB2 from Sedaoua; cf. Figs. 3 and 4). Each sample was divided into two parts: one for washing to search for foraminifera, and the other for preparing smear slides for

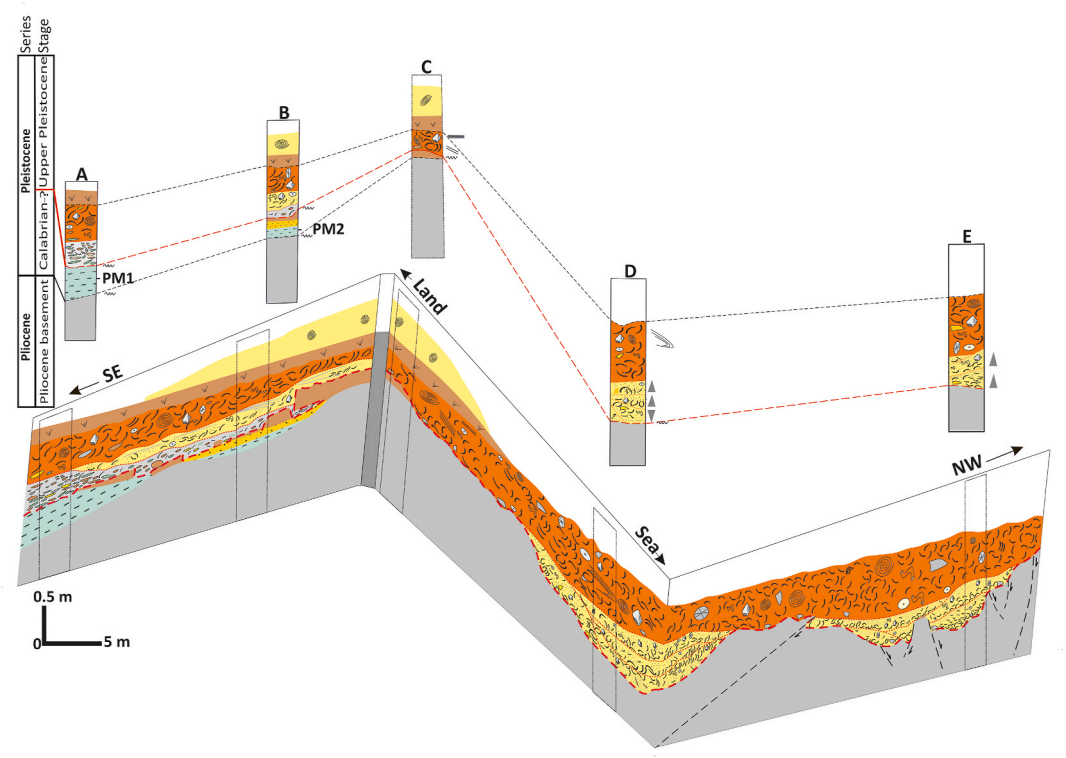

Fig. 4. Detail of the internal structure of the GRU unit at Port de Menard outcrop, showing the lateral variation in thickness and facies. Note the presence of an irregular erosion surface at the base of the *Glycymeris*-rich Unit at the contact with the Pliocene basement, Calabrian marls and paleosol, with positive and negative grading in the sub-layers. Same legend as in Fig. 3.

calcareous nannofossils. This approach completed the results obtained by Anderson (1936) and by Belkebir and Anglada (1985) and allowed dating the Pleistocene basement in this area with solid biostratigraphic evidence. The nannofossil slides were prepared using the short centrifugation technique as described by Bown and Young (1998). Each slide was observed at 1,600× magnification with an oil immersion lens under polarized light, using a Leica DM 2500P microscope. The extraction of planktonic foraminifera was carried out using a multistep process: initially, 200–300 g of sediment samples underwent deflocculation in lukewarm water to disaggregate the sediment matrix; following this, the sediment slurry was washed using a gentle stream of water through a 100 μm sieve to isolate the microfossil fraction.

Taxonomic analysis and identification of foraminiferal taxa were performed in two stages. The first stage was conducted in Algeria at the "*Laboratoire de Paléontologie Stratigraphique et Paléoenvironnement,*" where initial identifications were made using a binocular microscope with magnifications of 250 × and 500 × . The material was then transported to Bozok University in Turkey for advanced imaging and analysis. High-resolution images of the foraminifera were captured using a Scanning Electron Microscope (SEM), allowing for detailed examination of morphological features to confirm taxonomic identifications.

To determine the age of the *Glycymeris*-rich Unit (GRU), a variety of mollusc species (larger than 5 mm) were collected along the coastline of the Hachacha Plateau. The collected specimens were carefully washed and photographed in the MPB-Marine Palaeontology and Biogeography Laboratory at the University of the Azores. For taxonomic identification, the World Register of Marine Species (WoRMS) database (http://www.marinespecies.org) was used as a reference for accurate and standardized taxonomic attributions. This molluscan assemblage belongs to a group known as the Senegalese fauna, and indicates a warm period during the late Pleistocene (Ávila et al., 2002, 2007, 2009; Melo et al., 2023). According to Cornu et al. (1993) and Meco et al. (2002), the presence and development of the Senegalese fauna were associated with specific environmental conditions, particularly sea surface temperatures comparable to those currently observed in the Gulf of Guinea. These conditions require temperatures of approximately ~23 °C for at least six months per year, with the fauna exhibiting a limited tolerance for temperatures dropping below ~15 °C. In the Western Mediterranean, bio-stratigraphic correlations involving Pleistocene deposits containing Senegalese fauna are widely documented (Cerrone et al., 2021).

4. Results

4.1. Sedimentological characteristics and stratigraphy

Along 45 km of the coast of the Hachacha Plateau, chaotic marine sedimentary deposits unconformably overly Miocene, Pliocene, and Pleistocene basements though an irregular erosion surface. These deposits are rich in allochthonous molluscs, with abundant disarticulated bivalves and fewer gastropod remains within a conglomerate of pebbles to boulders. The fossiliferous sediments are exposed as 0.3 to 2.0 m-thick layers forming the GRU, the shells are randomly dispersed, in a sandy matrix agglutinated by a carbonate cement with no preferential orientation. Alongshore, from East to the West, a significant lateral variation is observed, especially in sedimentological composition (cf. Figs. 3 and 4). This variation is due to the depositional architecture, mainly deriving from the facies and palaeorelief of the basement, as well as to the local erosional base.

At Port de Menard (Eastern section of Hachacha Plateau; cf. Fig. 3), these deposits are located 4 m above present sea level, and represented by a thick (0.3–2 m), channelized GRU overlying the Pliocene sandstones of Hachacha through an angular unconformity (Belkebir, 1986). This formation is easily recognizable by a dense shell concentration, with excellent to good fossil preservation, in a yellow to red sandstone matrix. Shell concentration is organized in two to four sub-layers, either chaotic (especially the top sub-layer) or normal to reverse graded, and presents a lens-shaped geometry thinning out over distances of 2–3 m.

Shells are scarcer and more frequently broken within the channels and near the erosive surface, whereas towards the top they are generally intact and abundant (Fig. 5E). In some areas, above the Pliocene basement and below the GRU, marl lenses with a paleosol developed on top are present. Downward injections of sediment from the GRU intruded into this paleosol, locally detaching it (Fig. 5C). The lower sub-unit has a low faunal abundance, the shells are broken and presents a clay layer, transitioning laterally into a facies rich in rip-up clasts of paleosol and mud clasts from the underlying Calabrian marl (Fig. 5D). Thirty meters to the West, the facies vary, displaying sedimentary structures such as horizontal and oblique laminations and high-energy flow soft-sediment deformation structures (SSDS) (Fig. 5B). The upper 30 cm of this unit is a reddish shelly sandstone, containing continental snails mixed with marine shells (Fig. 5E–G). Its 10 cm-thick reddish undulated top layer contains rhizoliths, i.e., traces of plant roots.

At Sidi El Adjel beach, 1 km to the West, the GRU deposits truncate the Pliocene basement. It presents a lower sub-unit formed by a matrix-supported conglomerate with poorly sorted metric angular boulders from the basement and is poor in fossils. Locally, the deposit presents upwards fining and hydrodynamic structures such as parallel laminations and hummocky cross-stratification (HCS) (Fig. 6A).

At the Ain Brahim site, the studied succession crops out 1 m above present sea level, resting on a Pleistocene sandstone rich in SSDS (Fig. 6D and E) through an irregular erosive surface. It consists of two sub-units: a lower conglomeratic sub-unit, containing a few angular boulders and abundant mollusc shells; and an upper laminated sandstone sub-unit, interpreted as deposits from high-energy flow. In some places, these two sub-units are merged, forming a single unit that contains shells, generally dissolved and represented by internal moulds (Fig. 6F). The sequence is capped by aeolian deposits (Fig. 6D–G).

At Sedaoua, about 2 km to the West of the Ain Brahim site (Fig. 1), the GRU crops out 7 m above present sea level (Fig. 3). It stands on an erosion surface cut in a faulted basement formed by 1.5 m of Calabrian marl and bioturbated sandstones, which overlie Pliocene sediments (Fig. 7A–D). Its characteristics are like those observed at Port de Menard, especially the sedimentological features and faunal content, such as the coexistence of coralline algae, sponges and whole or slightly broken shell valves.

In Kef Boughetar area, the GRU stands 10 m above the present sea level (Fig. 3) on an erosion surface carved into the faulted Miocene sandstone basement (Fig. 7G). The deposit is 0.5–2.0 m-thick and consists of a chaotic conglomerate formed by centimetric to metric angular blocks of sandstone from the Miocene basement, rounded pebbles, and mud clasts in a sandstone matrix. The blocks are imbricated indicating transport to the NE. It contains gastropod and disarticulated bivalve shells and rounded bioeroded boulders (Fig. 7F). The shells in this unit are generally well preserved (Fig. 7H), being especially abundant in the gravelly pockets, but in places, they were almost completely dissolved.

Fig. 5. Representative photographs of the Port de Menard area. **A.** Pliocene basement faulted and overlain by the *Glycymeris*-rich Unit (GRU), with three sub-layers showing normal and reverse grading in the channelled base. **B.** Sedimentary features of the GRU, include horizontal and oblique laminations, and high-energy flow structures. **C.** The base of the GRU displays downward injections of the GRU sediment into and beneath the underlying paleosol. S.E.S. = Subaerial erosion surface. **D.** Detailed of the sub-layer rich in rip-up clasts (including paleosol and mud clasts) overlying a paleosol developed on Calabrian marl. **E.** Detail of the dense stacking of shells at the upper sub-unit of the GRU and the reddish sandstone matrix. **F, G.** Detail of terrestrial pulmonate gastropods mixed with the marine shells.

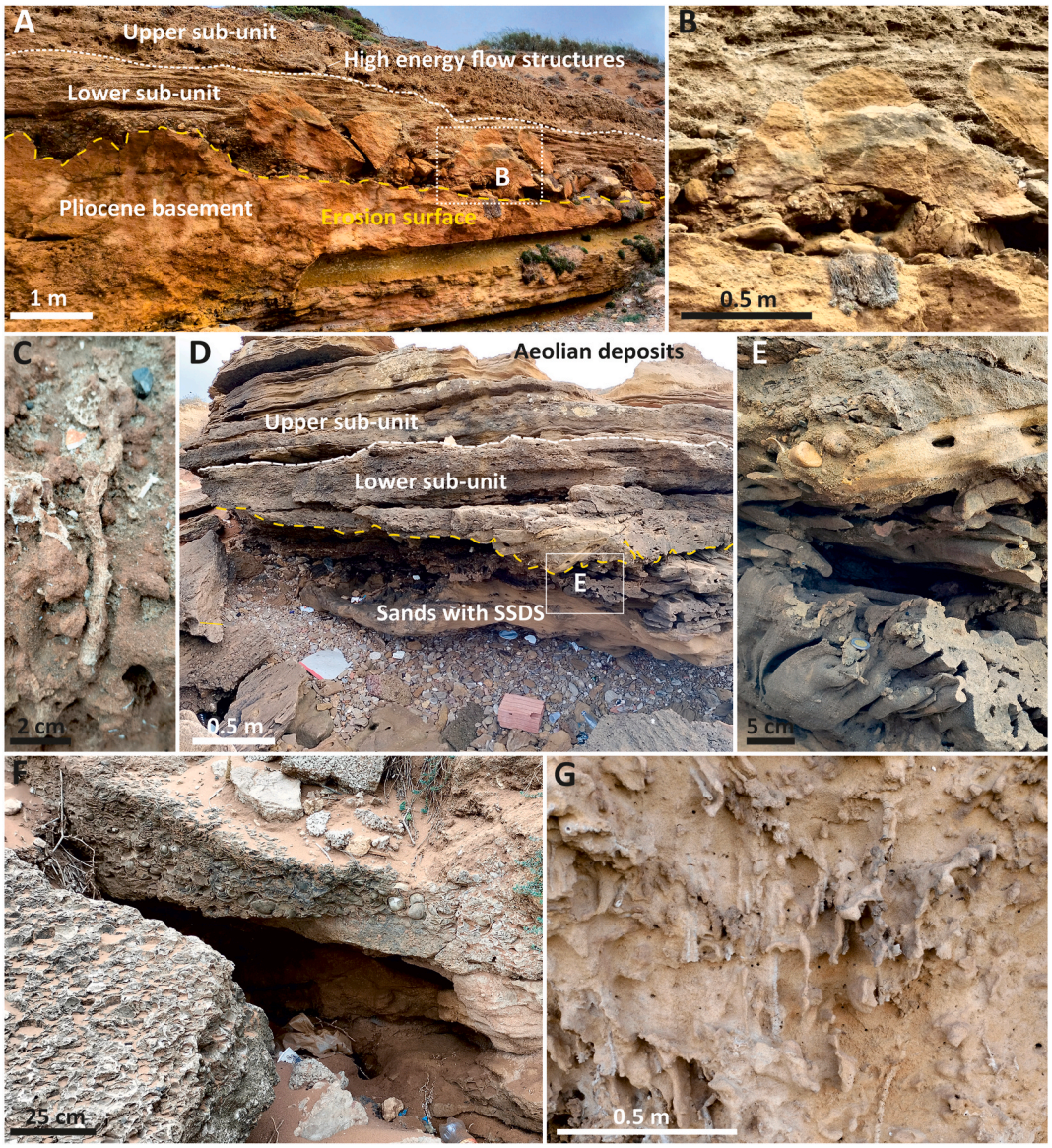

Fig. 6. A–E. Photographs of the Sid El Adjel section. **E–G.** Photographs of the Ain Brahim section. **A.** The GRU is composed of two sub-units; the lower one is a conglomeratic layer composed of large (m-sized) angular boulders eroded from the basement, containing few shells. The upper sub-unit is a finer conglomerate whose base show high-energy flow structures. The shells are nearly all dissolved and are represented by internal moulds. **B.** Detail of a fractured boulder that has not been totally separated from the basement **C.** Trace of a plant root (rhizolith) found at the top of the upper sub-layer. **D.** General view of Ain Brahim section show the presence of two sub-unit. **E.** Detail of the SSDS recorded in the contact between the GRU and the Pleistocene basement. **F.** GRU formed by a single unit in Ain Brahim area that contains shells dissolved and represented by internal moulds. **G.** Aeolian deposits with rhizoconcretions overlying the GRU at the Ain Brahim section.

Veins of calcite, probably from the dissolution of the shells, cross the more lithified parts of the deposit. The shells are more abundant at the top, as the sediment matrix becomes finer. The top of the deposit is pedogenized by caliche (Fig. 7H).

4.2. Biotic composition and taphonomy

Most of the macrofauna that makes up this shell bed is composed of bivalve molluscs. The dominant species is *Glycymeris*, with *Glycymeris nummaria* (Linnaeus, 1758) ranging from 61.6 to 84.9 %, along with *Acanthocardia echinata* (Linnaeus, 1758) (5.3–13.2 %) and *Anadara gibbosa* (Reeve, 1844) (1.0–4.3 %). *Chamelea gallina* (Linnaeus, 1758) (0.0–4.7 %), *Pecten jacobaeus* (Linnaeus, 1758) (0.0–2.9 %), and Ostreidae with *Ostrea edulis* Linnaeus, 1758 (0.0–1.9 %), are also present, but in smaller percentages (Table 1; Fig. 8). *Venus nux* (Gmelin, 1791) is absent from all samples except for the PMS1 and PMS4 squares (0.4–0.7 %) from the Port de Menard outcrop. Gastropods are represented by 14 taxa (Fig. 9), the most abundant being *Conus guanche* (Lauer, 1992), *Monoplex trigonus* (Gmelin, 1791) [= *Cymatium ficoides* (Reeve, 1844)], *Thetystrombus latus*, *Stramonita haemastoma* (Linnaeus, 1767), *Bolinus brandaris* (Linnaeus, 1758), *Steromphala adansonii* (Payraudeau, 1826) [= *Gibbula adansonii* (Payraudeau, 1826)], *Naticarius stercusmuscarum* (Gmelin, 1791), and *Tritia* cf. *elata* (A. Gould, 1845), with percentages ranging from 3.1 to 14.8 %. Other accessory elements are also present, such as serpulids (0.0–6.9 %), sponges (up to 2.2 %), corals and coralline algae forming rhodoliths (0.0–1.7 %) (Table 1).

Q-mode analysis of shell size and taphonomic characteristics of 13 sample squares revealed three distinct clusters (A, B, and C) with similar shell size and taphonomic criteria, but differing in fragmentation rate, organism interactions (boring), and number of shells analysed (Fig. 10). In terms of shell size, all sampled sites display good mechanical sorting,

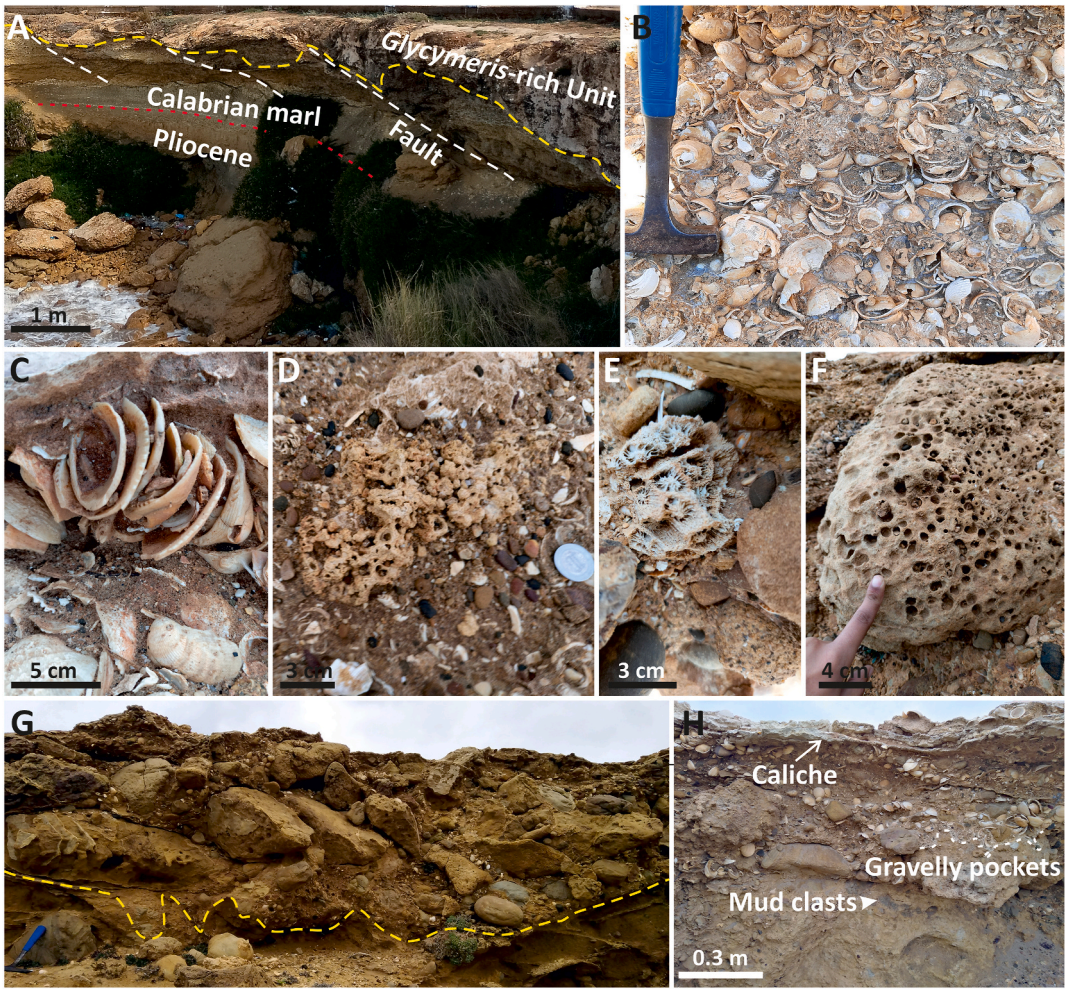

Fig. 7. A–**D.** Photographs of Sedaoua section. **E**–**H.** Photographs of Kef Boughetar section. **A.** General view of Sedaoua section. **B.** GRU of Sedaoua section with sponges and coral **C.** *Glycymeris* shells are arranged vertically, like plates in a dishwasher. **D.** Coralline algae in the Sedaoua section. **E.** Unidentified coral from the Kef Boughetar section **F.** Rounded marine boulder with *Gastrochaenolites* (bivalve borings). **G.** General view of the chaotic conglomerate deposits including mud clasts, boulders and gravely pockets, containing *Glycymeris* shells. Note the imbrication of the blocks of Miocene sandstone. Here, the GRU stands on an erosion surface carved on the Tortonian (Miocene) basement (yellow dashed line). **H.** A thin caliche is developed on top of the GRU.

Table 1
Relative abundance of the biotic components per square meter sampled, expressed as percentage. PMS – Port de Menard Surface, KBS – Kef Boughetar Surface.

Surface	Number of Shell	*Glycymeris* sp	*Acanthocardia echinata*	*Anadara gibbosa*	*Pecten jacobaeus*	Ostreidae	*Venus nux*	*Chamelea gallina*	Gastropods	Serpulids	Corals	Sponges
PMS1	282	81.9	5.3	1.4	0.7	0.4	0.4	0.7	4.3	2.1	1.1	1.8
PMS2	138	61.6	13.0	4.3	2.9	1.4	0.0	0.7	8.0	5.1	0.7	2.2
PMS3	162	82.7	6.2	4.3	0.6	1.9	0.0	0.0	3.1	1.2	0.0	0.0
PMS4	288	72.6	6.9	3.1	1.0	0.4	0.7	1.0	7.4	3.8	1.0	2.1
PMS5	223	79.4	5.8	2.2	0.0	1.8	0.0	0.9	8.1	1.4	0.0	0.4
PMS6	231	72.3	7.4	1.7	2.2	0.4	0.0	1.3	6.1	6.9	1.7	0.0
PMS7	86	79.1	8.1	0.0	0.0	1.2	0.0	4.7	6.9	0.0	0.0	0.0
KBS1	189	76.1	10.6	1.1	0.5	1.1	0.0	1.1	9.0	0.0	0.0	0.5
KBS2	122	67.2	12.3	0.0	1.6	0.8	0.0	0.8	14.8	1.6	0.8	0.0
KBS3	94	75.5	11.7	3.2	0.0	0.0	0.0	0.0	9.6	0.0	0.0	0.0
KBS4	182	64.3	13.2	0.5	0.5	1.7	0.0	2.8	11.5	3.3	1.1	1.1
KBS5	87	73.6	10.3	2.3	0.0	1.2	0.0	3.4	9.2	0.0	0.0	0.0
KBS6	93	84.9	5.4	0.0	0.0	0.0	0.0	2.2	6.5	0.0	0.0	0.0

with a predominance of valves measuring between 3 and 5 cm. Taphonomic results reveal a complete absence of articulation, with a low fragmentation rate in clusters B and C (2.1–16.2 %). On the other hand, Cluster A, comprising samples PMS7, KBS3, KBS5 and KBS6 located inside channels, where the deposit is coarser, shows moderate fragmentation close to the erosive surface (15.5–44.4 %) (Table 2).

As for the abrasion, the shells have dominantly sharp edges (53.6–76.4 %), while the percentage of rounded fractures is lower than 46.4 % on all squares. For organism interactions, clusters A and B show low percentages of borings, except in samples KBS5 and KBS6 from cluster A, which exhibit moderate percentages of bioerosion structures (16.8–22.9 %). Cluster C, comprising samples PMS1, PMS4, PMS5, and

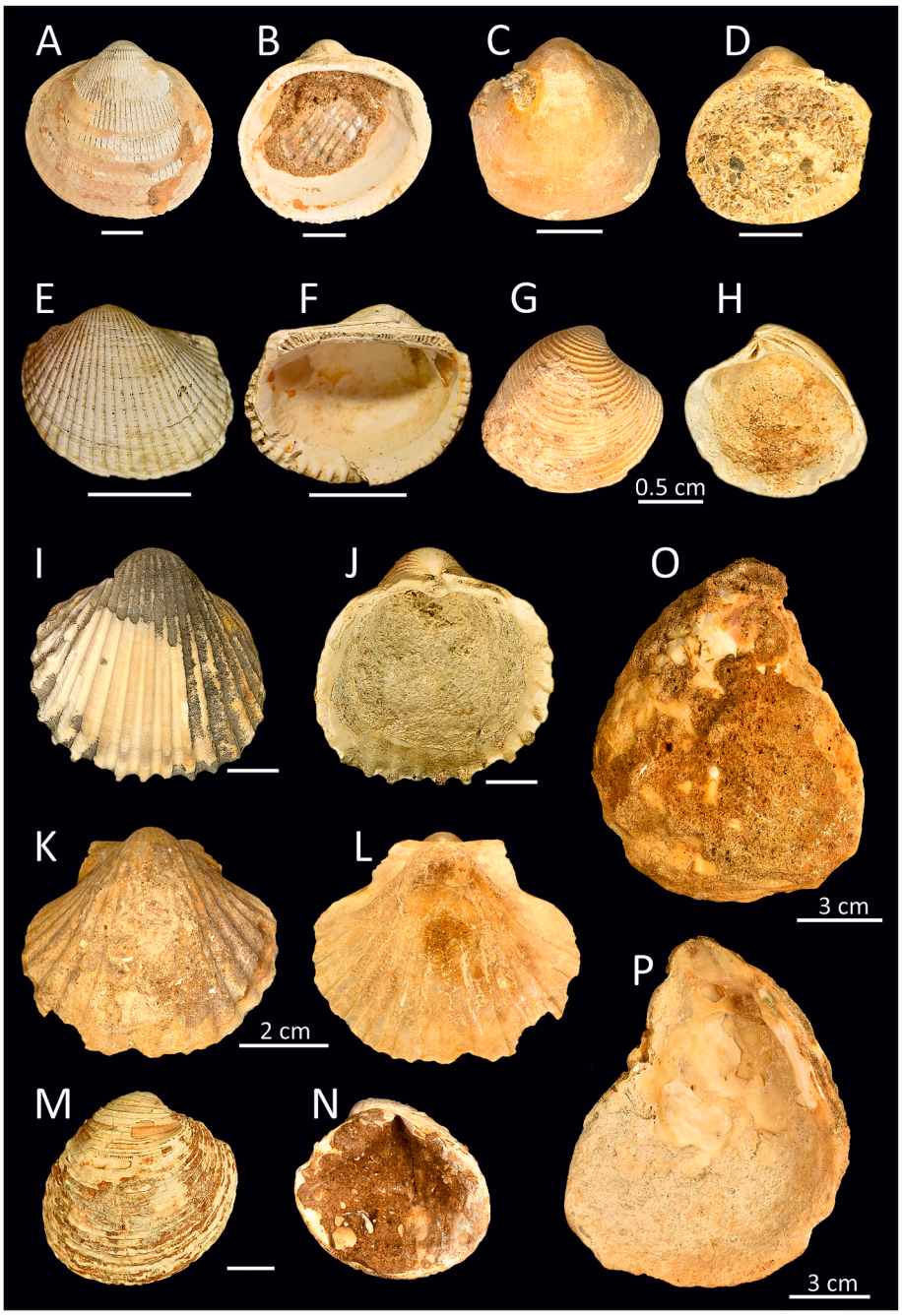

Fig. 8. Bivalve taxa from the upper Pleistocene of Hachacha Plateau. **A–B.** *Glycymeris* sp. **C–D.** *Glycymeris nummaria* (Linnaeus, 1758). **E–F.** *Anadara gibbosa* (Reeve, 1844). **G–H.** *Chamelea gallina* (Linnaeus, 1758). **I–J.** *Acanthocardia echinata* (Linnaeus, 1758). **K–L.** *Pecten jacobaeus* (Linnaeus, 1758). **M–N.** *Venus nux* Gmelin, 1791. **O–P.** *Ostrea edulis* Linnaeus, 1758. Scale bar = 1 cm for all unless otherwise specified.

PMS6 characterized by shells packed in a reddish sandstone matrix, shows very low percentage of borings (<4.6 %). Encrustation is reported in two samples (PMS7 and PMS4), with very low percentages of no more than 2.3 % (Table 2).

In vertical section, shells show oblique (30–60°) and perpendicular (60–90°) stacking orientation on all sampled surfaces, except for samples KBS3 and KBS5 from cluster A, which disclose a preferentially horizontal stacking orientation (0–30°), with percentages varying between 40.6 and 48.9 %. In terms of concavity orientation, all three clusters reveal comparable results, illustrating a predominance of shells oriented with their concave parts downwards, with percentages exceeding 50 % (Table 2).

4.3. Micro and nannofossil assemblages in the lenticular marl (Pleistocene basement)

The smear slide analysis of the lenticular marl sediment (LM), intercalated between the Pliocene and the *Glycymeris*-rich Unit, from Port de Menard (PM) and Ain Brahim (AB) (Figs. 3 and 4) yielded a total of 17 taxa of calcareous nannofossils. Of these, *Gephyrocapsa* (small), *Reticulofenestra* spp., and the extinct *Pseudoemiliania lacunosa* Kamptner ex S. Gartner were the most abundant in all four samples (PM1, PM2, AB1, and AB2). *Discoaster* spp. (also extinct), *Calcidiscus macintyrei* (Bukry and Bramlette) Loeblich and Tappan, *Gephyrocapsa* (large) and *Coccolithus miopelagicus* Bukry, 1971 are also present, albeit always in small percentages. The analyses of the planktonic foraminifera revealed

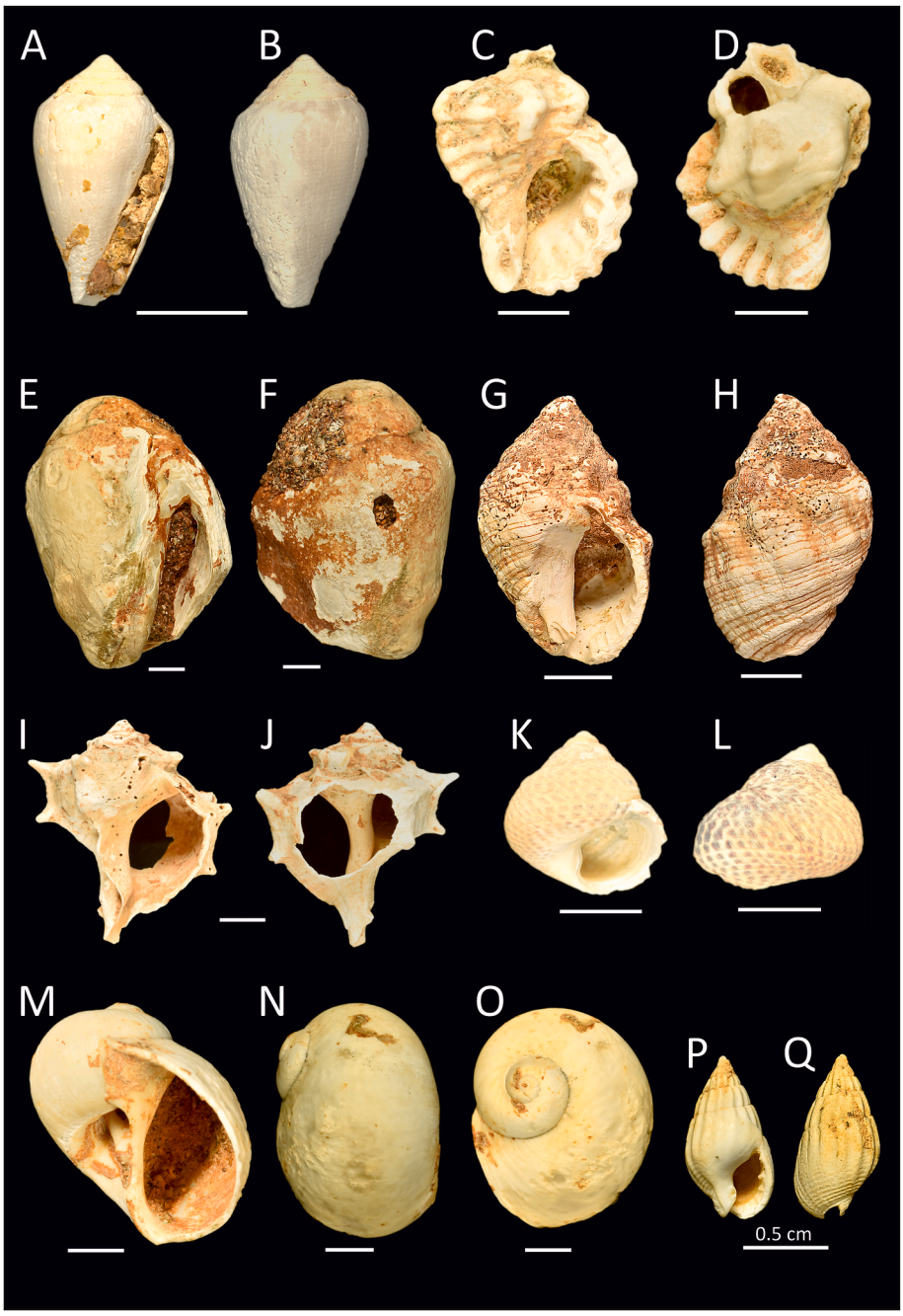

Fig. 9. Gastropods species from the upper Pleistocene of Hachacha Plateau. **A–B.** *Conus Guanche* (Lauer, 1993). **C–D.** *Monoplex trigonus* (Gmelin, 1791). **E–F.** *Thetystrombus latus* (Gmelin, 1791). **G–H.** *Stramonita haemastoma* (Linnaeus, 1767). **I–J.** *Bolinus brandaris* (Linnaeus, 1758). **K–L.** *Steromphala adansonii* (Payraudeau, 1826) [= *Gibbula adansonii* (Payraudeau, 1826)]. **M–O.** *Naticarius stercusmuscarum* (Gmelin, 1791). **P–Q.** *Tritia* cf. *elata* (Gould, 1845). Scale bar = 1 cm for all unless otherwise specified.

a diverse assemblage, with the notable presence of the species *Globoconella inflata* (d'Orbigny, 1839), which is the only planktonic foraminifera biomarker species identified in the lenticular marl.

5. Discussion

5.1. The age of the lenticular marl (lower Pleistocene basement)

According to Backman et al. (2012), the CNPL 9 biozone, also known as the *Small Gephyrocapsa* PRZ biozone (see Gartner, 1977), was defined on the basis of the presence of specific nannofossil species in the samples and is known for the virtual disappearance of medium (4.0–5.5 μm) and large (over 5.5 μm) *Gephyrocapsa* species, as noted by Rio (1982) and Raffi et al. (1993). The nannofossil assemblages of this biozone are characterized by the predominance of small-sized *Gephyrocapsa* and *P. lacunosa*, which has been observed in various oceans (Gartner, 1977; Rio, 1982; Raffi et al., 1993, 2006; Wei, 1993). The CNPL 9 biozone corresponds to the middle levels of Martini NN19 and was identified in all samples from the lenticular marl, being characterized by the partial range of the nominal taxon "*small Gephyrocapsa*", which lies between the top of *Gephyrocapsa* (large) and the re-entry of *Gephyrocapsa* (greater than 4 μm). This allows the attribution of an Early Pleistocene age (Calabrian; 1.25–1.06 Ma) to this unit.

Since *Globoconella inflata* (d'Orbigny, 1839) first appeared at 2.09

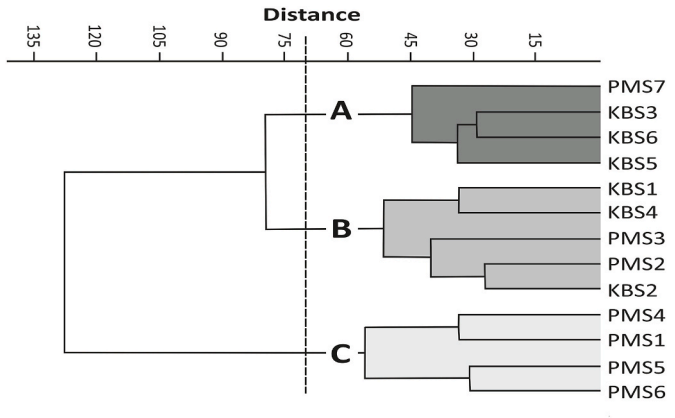

Fig. 10. Q-mode cluster analysis, with Unweighted Pair Group Method with Arithmetic mean (UPGMA), and Euclidean distances. PMS – Port de Menard Surface; KBS – Kef Boughetar Surface.

Ma in the Eastern Mediterranean Sea (Lourens et al., 2005), the foraminifera assemblage also supports an early Pleistocene age for the lenticular marl.

5.2. The age of the conglomeratic Glycymeris-rich unit (GRU)

The GRU crops out at elevations ranging from 1 to 10 m above the present sea level (cf. Fig. 3) and exhibits a remarkable diversity of gastropods, including *Conus guanche, Monoplex trigonus, Naticarius stercus-muscarum*, *Stramonita haemastoma*, *Bolinus brandaris*, *Tritia* cf. *elata*, and *Thetystrombus latus* (Fig. 9). Rare specimens of the coral *Cladocora caespitosa* (Linneaus, 1767) are also present. This assemblage of gastropods, along with *C. caespitosa*, is typical of the "Senegalese fauna" (Benjamin et al., 2017; Cerrone et al., 2021), which colonised the Mediterranean coasts during the Last Interglacial period (del Valle et al., 2024).

The term "Senegalese fauna" derives from the fact that its most characteristic species, the gastropod *Thetystrombus latus*, is currently found along the Atlantic coasts of West Africa, spanning from Senegal to Angola, as well as in the Cabo Verde Archipelago, i.e., in warm, low latitude regions. Last Interglacial deposits with elements of the "Senegalese fauna" occur throughout the Western Mediterranean, except for the coasts of the Northern Adriatic Sea (Cerrone et al., 2021). Last Interglacial deposits with "Senegalese fauna", are also know from the Atlantic archipelagos of the Azores (Ávila et al., 2010, 2015a, 2016, 2018, 2020; Madeira et al., 2007; Hyžný et al., 2021; Melo et al., 2023), Madeira (Gerber et al., 1989), Selvagens, Canaries (Meco, 1977; Meco et al., 1997) and Cabo Verde (Melo et al., 2022a, 2022b).

The presence of *T. latus*, *C. guanche* and *S. haemastoma* indicates shallow, warm marine waters, and an upper Pleistocene age (Gignoux, 1911; Bard et al., 1994; Kreipl and Poppe, 1999; Meco et al., 2002; Torres et al., 2006, 2010; Ramirez et al., 2009; Harzhauser and Kronenberg, 2013; Sessa et al., 2013; Muhs et al., 2014; Chakroune and Zaggbib-Turki, 2017). The occurrence of "Senegalese fauna"/*T. latus* in deposits of the Western Mediterranean Pleistocene is often used as an indicator of a Last Interglacial age (more precisely of its warmer period known as the MIS 5e). However, the accuracy of this chronological attribution has been questioned, particularly for the Mediterranean coasts of Spain. This is due to the discovery of *T. latus* on marine terraces dated not only to MIS 5e, but also to MIS 7 and MIS 9 (Zazo et al., 2003). Arguments against exclusively assigning deposits containing *T. latus* to MIS 5e were presented in comments (Mauz and Antonioli, 2009) and replies (Bardají et al., 2009b) to a paper by Bardají et al. (2009a). Nonetheless, there is a consensus that deposits containing the Senegalese fauna are assigned to the MIS 5e, the Last Interglacial period. This is because the faunal assemblage associated with "Senegalese fauna" is

Table 2
Values for the size sorting and taphonomic attributes, expressed as percentage, for the two sectors under study (Port de Menard and Kef Boughetar).

Surface	Number of shells analysed	Fragmentation			Shell size			Angle with stratification				Concavity orientation		Abrasion		Interactions		Articulation
		[0–10 %]	[10–50 %]	[50–90 %]	[1–3 [	[3–5 [	[5–7]	0–30°	30–60°	60–90°	Vertical	Up	Down	Edge ounded	Edge sharpe	Borings	Encrustation	
PMS1	254	80.2	16.7	3.1	21.2	62.7	16.1	26.1	30.4	43.5	15.3	38.8	61.2	35.8	64.2	4.6	0.0	0.0
PMS2	125	66.0	27.9	6.1	18.9	63.5	17.6	31.9	35.3	32.8	21.7	45.7	54.3	29.0	71.0	10.5	0.0	0.0
PMS3	145	55.8	32.4	11.8	25.1	56.4	18.5	23.8	31.9	44.3	13.7	34.3	65.7	37.6	62.4	8.7	0.0	0.0
PMS4	255	62.3	21.5	16.2	22.3	58.1	19.6	21.5	37.4	41.1	16.4	48.4	51.6	23.6	76.4	4.3	1.7	0.0
PMS5	195	79.3	15.6	5.1	20.4	53.9	25.5	25.6	30.8	33.7	18.5	47.6	52.4	43.2	56.8	3.6	0.0	0.0
PMS6	219	82.4	13.3	4.3	15.6	61.1	23.3	25.6	37.1	37.3	9.2	48.4	51.6	34.7	65.3	2.9	0.0	0.0
PMS7	80	20.1	35.5	44.4	22.1	58.4	19.5	32.7	31.1	36.2	14.2	37.0	63.0	46.4	53.6	6.9	2.3	0.0
KBS1	167	79.2	18.7	2.1	35.3	53.9	10.8	27.6	41.8	30.6	17.9	47.4	52.6	41.6	58.4	13.9	0.0	0.0
KBS2	109	57.8	35.8	6.4	32.0	58.2	9.8	30.0	36.3	33.7	19.1	44.7	55.3	34.6	65.4	14.5	0.0	0.0
KBS3	84	35.2	40.5	24.3	25.5	68.6	5.9	40.6	27.3	32.1	5.2	41.3	58.7	36.0	64.0	5.7	0.0	0.0
KBS4	156	65.2	23.7	11.1	28.8	67.6	3.6	38.3	33.1	28.6	3.0	48.6	51.4	42.7	57.3	11.8	0.0	0.0
KBS5	75	35.5	42.3	22.3	42.0	53.6	4.4	48.9	33.6	27.5	10.1	38.9	61.1	38.0	62.0	16.8	0.0	0.0
KBS6	80	40.4	44.1	15.5	23.4	70.3	6.3	30.2	36.0	33.8	13.9	48.8	51.2	31.9	68.1	22.9	0.0	0.0

present throughout the Western Mediterranean for the entire duration of the MIS 5e (Cerrone et al., 2021). In the Canary Islands, all deposits with *T. latus* are also assigned to the MIS 5e (Meco, 1977; Meco et al., 1997; Martín-González et al., 2019). Therefore, based on the fossil molluscs' assemblage (associated with the Senegalese fauna), we attribute an upper Pleistocene (MIS 5e) age to the GRU deposits.

5.3. GRU depositional model

The presence of Senegalese fauna within the *Glycymeris*-rich Unit has allowed these deposits to be more effectively correlated along the coastline of the Hachacha Plateau. The studied unit is characterized by an assemblage of shells that are allochthonous, disarticulated, and well-sorted. Forming a densely packed unit (*sensu* Kidwell et al., 1986) dominated by *Glycymeris* spp., these features suggest that hydraulic energy is the primary factor controlling the concentration of skeletal remains (Kidwell et al., 1986; Davies et al., 1989; Dattilo et al., 2008). Mud clasts, rip-up clasts of soil, and angular boulders are derived from the erosion of different basement units (Miocene, Pliocene, and Pleistocene) present in the study area, while the bioeroded boulders, rounded pebbles, and the sand matrix indicate a marine origin. This suggests that an extreme event such as a tsunami or storm was responsible for the sediment transport and deposition.

The lateral variation in facies and thickness due to geomorphological factors and variable basement rocks, along with sedimentary structures such as hummocky cross-stratifications (HCS), parallel or oblique laminations, and imbricated boulders, combined with an erosional base, indicate deposition in a dynamic, high-energy coastal environment (foreshore/backshore), while the Senegalese fauna content indicates a warm climate. The good preservation of the shells, along with a low percentage of biotic interactions, implies rapid burial and short exposure on the seafloor, or to the wave action (Donato et al., 2008; Dawson and Stewart, 2007). This suggests transport mostly beyond the foreshore, and further inland to the backshore zone during an extreme inundation event.

At Port de Menard, overlying the Calabrian marl, a sub-unit contains abundant mud and paleosol clasts ripped-up from the basement, and mud layers interpreted as decantation of stagnant muddy water (Fujiwara and Kamataki, 2007) (Fig. 5D). These features indicate that lateral facies variation is related to the nature of the eroded basement and local geomorphology. In this area, the Pliocene basement exhibits channels parallel to the shoreline. These channels, locally controlled by faults, may result from the erosive action of an extreme wave event (Figs. 4 and 5A). This process favoured the capacity to accommodate a considerable volume of bioclastic materials in the coastal environment. Inside these channels, three sub-units display alternating normal and reverse grading. This grading pattern indicates that sediment was transported in suspension under turbulent flow conditions. These high-energy flow conditions are also supported by the occurrence of horizontal and oblique laminations in another channel (Fig. 5B). Other channel deposits, forming a lower sub-unit at Sid El Adjel, are characterized by a matrix-supported conglomerate with m-sized angular boulders, eroded from the Pliocene basement (rocky coast), imbricated above the irregular erosive surface (Fig. 6A). The presence of a boulder that has been levered but not completely separated from the basement indicates that these large angular blocks were locally quarried from the basement and incorporated in the transported mass of sediment (Fig. 5A–C).

At Port de Menard, a paleosol is partially preserved below the GRU indicating that this unit was deposited inland, possibly at the backshore. Approximately 40 m inland, the marine sediment is injected into and below the paleosol (Figs. 4 and 5C) and includes friable rip-up clasts of the soil. Another evidence of terrestrial deposition is the presence of terrestrial molluscs mixed with the marine shells in the reddish shelly sandstone upper layer. This suggests that this sub-layer represents a backwash unit, which incorporated terrestrial sediment (red soil clay) and fauna. The presence of a thin paleosol with plant root traces and aeolian deposits overlaying the GRU unit, supports the interpretation of a subaerial exposure of the GRU sediment after deposition (Fig. 6C).

In the Ain Brahim area, the GRU consists of two sub-units, suggesting deposition by different waves. The upper laminated sandstone possibly represents a wave coming from a different direction that essentially transported sand. The local dissolution of the shells in this area is probably recent and related to the direct exposure of the deposits to waves or to marine spray, which not only physically erodes the material but also promotes chemical interaction between the shells and the acidic seawater (Duquette et al., 2017; Barclay et al., 2020). The soft sediment deformation structures found within the underlying Pleistocene basement are interpreted as seismite structures (Fig. 6E) resulting from seismically induced liquefaction (Buchner et al., 2021). These structures were reported by Guessoum et al. (2018) from several areas of the Lower Chelif Basin and are attributed to earthquakes of magnitude $M > 5.5$.

The Sedaoua section represents one of the most complete marine Pleistocene series in the Northern part of the Hachacha Plateau. The stratigraphic succession consists of lenticular marl, sands, and bioturbated sandstone from the Pleistocene basement, overlain by the GRU deposits. These deposits exhibit a mixture of organisms from different shallow marine environments, including bivalves, gastropods, corals, coralline algae forming rhodoliths, sponges, and serpulids. This suggests that the marine remains were transported from the shoreface towards the coastal zone (transfer environment) during an extreme event.

The GRU in the Kef Boughetar region is deposited unconformably atop the faulted Miocene basement (Tortonian), reflecting a dynamic depositional history shaped by both tectonic and sedimentary processes. These deposits, dominated by *Glycymeris* shells, exhibit large imbricated angular boulders (from the Tortonian basement) and other rip-up clasts (mud clasts). These characteristics suggest a deposit related to an extreme event, with high-energy condition, and a substantial supply of sediments, which contributed to the accumulation of this diverse material in the coastal area. At Kef Boughetar, the outcrop of the GRU stands at an elevation of 10 m above the present sea level. The faults affecting the Miocene basement likely created zones of weakness which facilitated the removal of boulders by the waves and influenced the localization and geometry of subsequent sedimentary deposits.

5.4. Deposition processes: tsunami or storm

Both tsunamis and storms can produce shell beds with distinct sedimentological and taphonomic characteristics. Recently, these skeletal concentrations have been used to identify the processes responsible for their formation in marine environments ranging from onshore to offshore (Puga-Bernabéu et al., 2007; Donato et al., 2008, 2009; Morales et al., 2008; Massari et al., 2009; Reinhardt et al., 2012; Puga-Bernabéu and Aguirre, 2017; Khadraoui et al., 2018; Torres et al., 2022), or within lacustrine systems (Sztanó et al., 2020; Naimi et al., 2023; Rodrigues et al., 2024).

The biotic association characterizing the GRU is defined by the presence of taxa spanning a wide ecological range, from supralittoral to infralittoral zones, with occasional representation of organisms indicating a shallow circalittoral biocenose. The assemblage includes *Glycymeris* ssp., *G. nummaria*, *A. echinata*, *A. gibbosa, V. nux*, *P. jacobaeus*, and *C. gallina*, organisms reported in Mediterranean infralittoral to shallow circalittoral biocenoses. *Venus nux*, inhabiting depths between 10 m and 700 m, is associated with sandy mud to muddy sand, while *P. jacobaeus* occurs at depths ranging from 9 to 250 m in substrates ranging from coarse sand and gravel to fine sands and muddy sands. *Chamelea gallina*, typically found between 2 and 60 m, occupies fine sand, sandy mud, and muddy sand habitats. These features combined with the low percentages of boring and the total absence of encrustation, along with a good to excellent shell preservation, suggest that extremely powerful waves reaching deep areas beneath the taphonomic active zone eroded sediment masses that buried the shells (Donato et al., 2009;

Massari et al., 2009). Our results reveal a predominance of sharp-edged fragmentation surfaces. According to Donato et al. (2008), this characteristic is one of the most significant indicators of skeletal remains associated to tsunami events, a finding that was also proposed by other studies (Puga-Bernabéu and Aguirre, 2017; Khadraoui et al., 2018).

The chaotic arrangement of shells, with a dominance of elements oriented obliquely to vertically (30–90°) (Table 2), often stacked in a manner resembling plates in a dishwater (Fig. 7C), suggests transport within a mass flow (Puga-Bernabéu and Aguirre, 2017). This mode of transport minimizes strong impacts between reworked bivalves (Massari et al., 2009), preserving them. This interpretation is further reinforced by the presence of sedimentary structures indicative of high-energy depositional processes. These high-energy flow structures, combined with the chaotic texture of the deposit and presence of both soft and hard-rock rip-up clasts (Fig. 5B and 6A), suggest rapid, dynamic, and energetic sediment erosion and transport associated with mass flows and are typically associated with tsunamis. The angular blocks ripped-up from the lithified basement rocks, together with soft sediment clasts, embedded within the matrix of the deposit, imply a high-energy, non-selective transport mechanism capable of entraining and depositing both fine-grained sediments and large clasts together (Fig. 6A and 7G), while preserving delicate clasts of soil. Such conditions are typical of catastrophic depositional events, where the extreme energy of the flow rapidly mobilizes and reworks sediments from diverse environments in a chaotic manner (Scheffers et al., 2009). Another feature observed in at least two outcrops is the clear imbrication of these blocks, indicating a Northeastward current. All these features, reflect intensive and rapid depositional processes, distinguishing these deposits from those formed in more gradual or oscillatory flow conditions, such as those associated with storm events (Rossetti et al., 2000). The presence of both fragile soil and hard-rock rip-up angular clasts in the lower part of the GRU and near the erosion surface in Kef Boughetar and Port de Menard areas (Fig. 5D and 7H), indicate the action of turbulent water triggered by the first wave(s) of this extreme event/tsunami. These waves eroded the pre-existing deposits, producing the observed clasts. Another characteristic is the occurrence of sediment injections into both hard and soft substrates reported from several tsunami deposits (Paris et al., 2018; Madeira et al., 2020), that in some cases illustrate the process of erosion and quarrying of the basement. Such features are commonly associated with the sedimentary record of tsunami events, as documented in numerous studies (Gelfenbaum and Jaffe, 2003; Goff et al., 2004; Morton et al., 2007; Matsumoto et al., 2010; Ramalho et al., 2015; Khadraoui et al., 2018; Paris et al., 2018; Madeira et al., 2020). In contrast, soil rip-up clasts are absent and muddy rip-up clasts are rarely reported in storm deposits (Morton et al., 2007).

The good sorting, with a predominance of 3–5 cm valves, is one of the most distinctive features of the GRU. This can be explained by the low percentage of fragmented shells, as high fragmentation typically produces sedimentological skeletal concentrations with varying sizes, resulting in poorly to moderately sorted coquinas (Puga-Bernabéu and Aguirre, 2017). The occurrence of articulated bivalve shells in non-living position is often considered indicative of shells transported while still alive during tsunami events (Donato et al., 2008; Massari et al., 2009; Ando et al., 2018; Kitamura et al., 2018; Madeira et al., 2020). However, the studied unit exhibits a total absence of articulated bivalves, a feature that is more common in tsunamigenic deposits, both in coastal (Torres et al., 2022) and offshore settings (Puga-Bernabéu and Aguirre, 2017). Regarding the shells concavity, our results indicate that among the horizontally oriented shells (0–30°), those with concavity-down orientation, dominate across all measured samples, with percentages ranging between 51.2 % and 65.7 % (Figs. 11–13). These is consistent with the results of Puga-Bernabéu and Aguirre (2017), who also reported a predominance of concavity-down shells within tsunami deposits. This pattern contrasts with storm deposits, which are dominated by shells in a concave-up orientation.

Massari et al. (2009) reported the presence of normal and inverse grading within tsunamis deposits, linked to deposition from prolonged high-energy sediment flow. The fining-upward texture and stacking of sub-layers with inverse and normal grading has also been reported in tsunami deposits at different locations (Fujiwara et al., 2003; Paris et al., 2018; Madeira et al., 2020). Additionally, the imbrication of large boulders is another key feature often linked to tsunami events (Goto et al., 2007; Scicchitano et al., 2007; Maouche et al., 2009; Barbano et al., 2010; Paris et al., 2011, 2018; Sugawara et al., 2014; Brill et al., 2017; Madeira et al., 2020). As noted above, the variation in facies and thickness is influenced by the pre-existing topography and lithologic nature of the affected areas. Hori et al. (2007) reported that thick tsunami sediments tend to accumulate in channels, as observed during

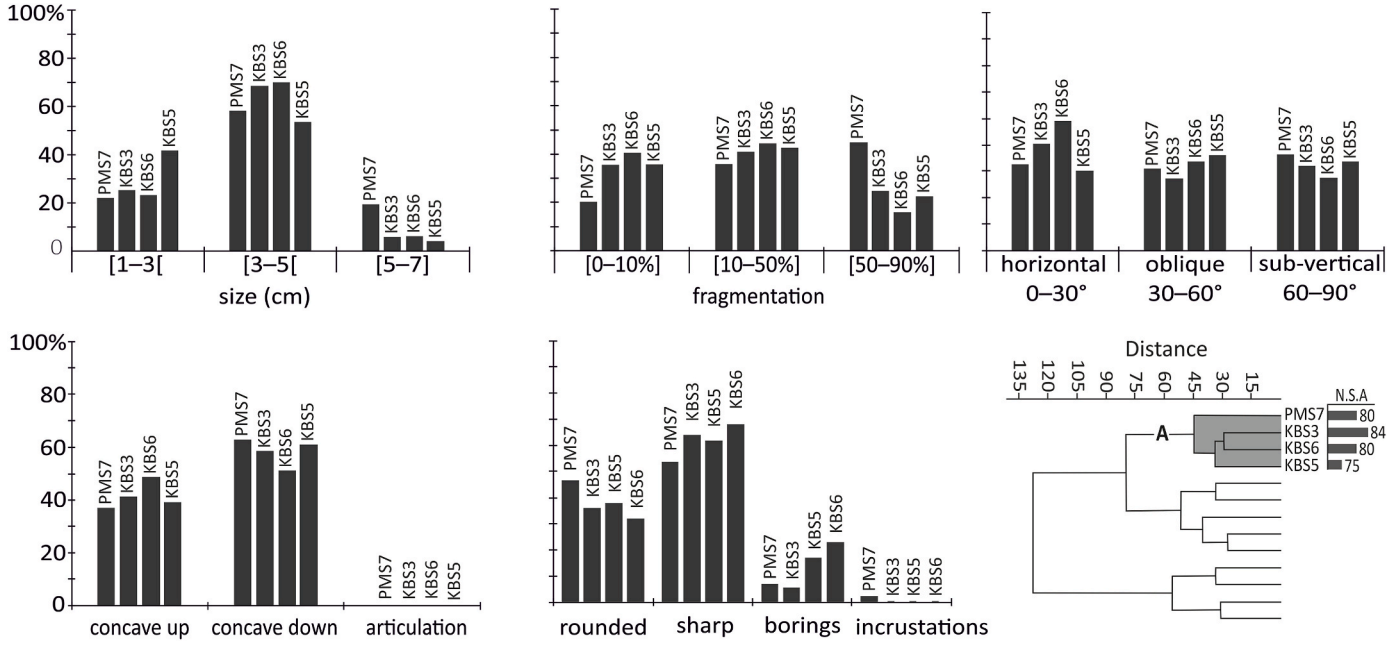

Fig. 11. Histograms of size sorting and taphonomic attributes characterizing cluster A. PMS – Port de Menard Surface; KBS – Kef Boughetar Surface. NSA – Number of shell analysed.

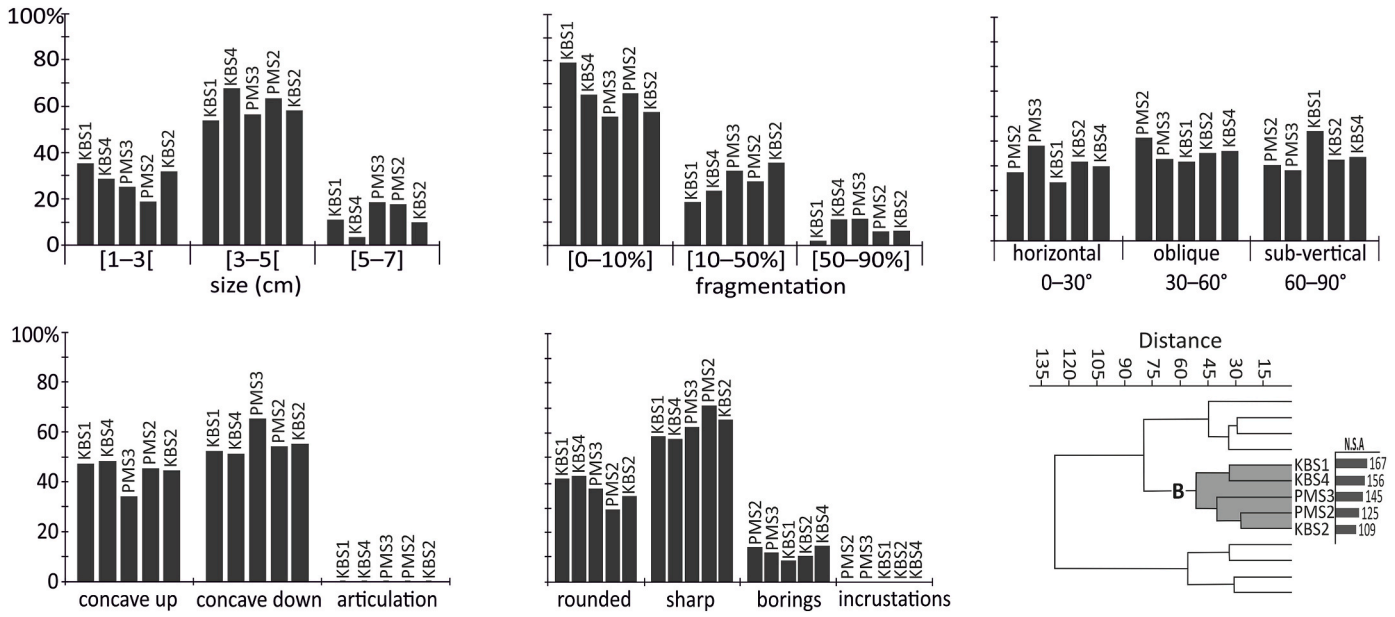

Fig. 12. Histograms of size sorting and taphonomic attributes characterizing cluster B. Abbreviations as in Fig. 11.

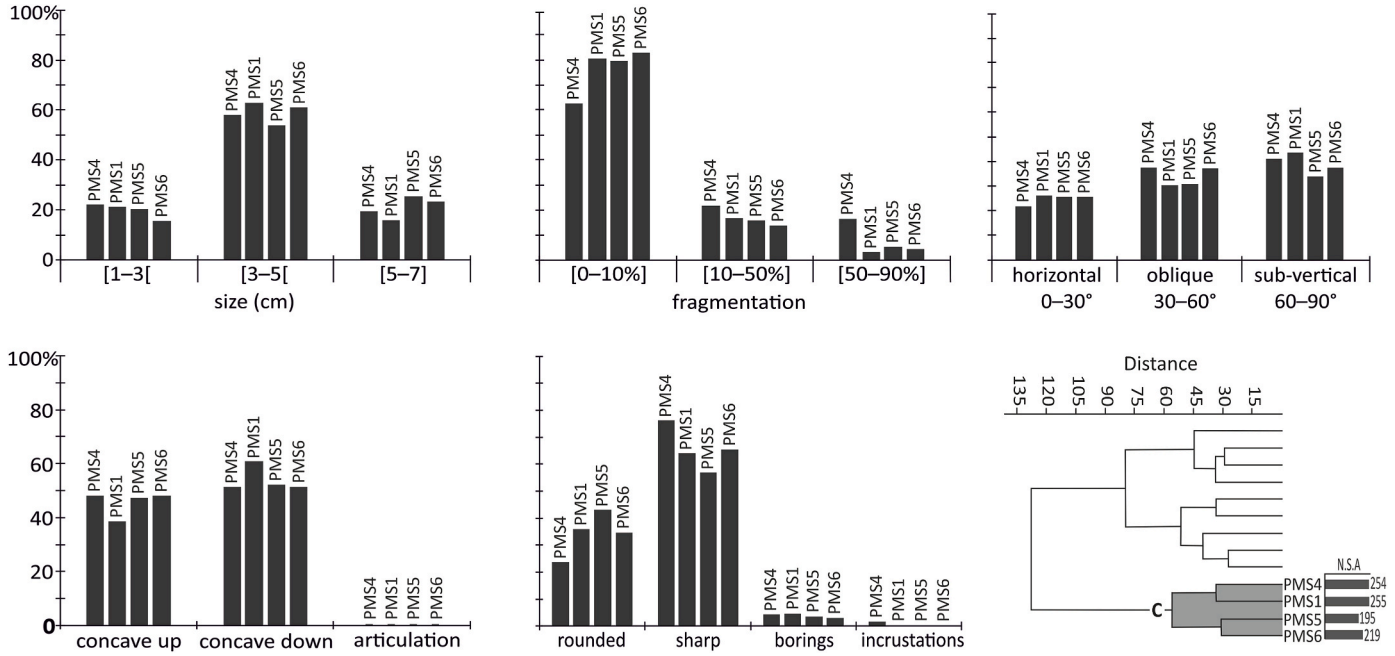

Fig. 13. Histograms of size sorting and taphonomic attributes characterizing cluster C. Abbreviation as in Fig. 11.

the 2004 tsunami that impacted the West coast of Thailand. In contrast, sediments are thinner in areas with local convex topography. Nishimura and Miyaji (1995) also emphasized that the thickness of sediment layers generated by a tsunami event is controlled by the topographic undulations. This observation aligns with findings from the two localities of Port de Ménard and Sid El Adjel, where the deposits of the studied unit overlie the Pliocene basement, which exhibits channels parallel to the shoreline that accommodate a considerable volume of sediment, with maximum thickness observed.

In summary, our analysis suggests that the GRU was deposited on land by a tsunami event during the MIS 5e. Supporting this hypothesis is the evidence provided by the presence of terrestrial deposits both underlying and overlying the studied unit, as well as the mixture of terrestrial and marine sediment and shells.

5.5. *Triggering mechanism*

From a structural point of view, Northwestern Algeria belongs to the Tellian Atlas, at the boundary between the African and Eurasian tectonic plates. This region is one of the most seismically active zones in the Western Mediterranean (Maouche et al., 2019). Notable examples of significant seismic events include the El Asnam earthquake (M = 7.1), which resulted from a 36 km-long surface rupture of a thrust fault (King and Vita-Finzi, 1981; Philip and Meghraoui, 1983). Other notable seismic events include the Tenes earthquake in 1992 (M = 5.8) and the Zemmouri earthquake on May 21, 2003 (M = 6.9) (Ayadi et al., 2003; Meghraoui et al., 2004).

This seismic activity is linked to active compression, producing NE–SW to E–W trending folds and associated faults (Maouche et al.,

2019). Unfortunately, the presence of this neotectonic deformation does not allow us to estimate uplift or subsidence rates for the deposition sites. On the Hachacha plateau, several canyons, including Kramis, Zarifa, Roman, and Abid (Fig. 1), are controlled by strike slip faults. These faults have been reactivated during the Quaternary period and produced landslides in the margins of Dahra Massif (Matougui and Haddoum, 2008). In this context, we consider that the GRU is probably associated with the active tectonics in the region. This assumption is supported by the extensive network of faults affecting the Quaternary sedimentary cover in the offshore (Matougui and Haddoum, 2008) (Fig. 1). According to the interpretation of the seismic line (SPI-O2 profile) by Badji et al. (2015) and Soto et al. (2022) (Fig. 2), salt tectonics affecting the seafloor is another possible source, such as the Ameur salt wall (Ameur Diapir) that disrupts recent Quaternary deposits. Vannucci et al. (2004) concluded that the Algerian offshore is the main source of seismic activity triggering tsunami events in the Western Mediterranean and, according to Roig-Munar et al. (2023), the historical earthquakes off the Algerian coast between 1365 and 2023 produced most of the tsunamis recorded in the Western Mediterranean, especially in Southern Spain.

The occurrence of SSDS in Ain Brahim area within the Pleistocene basement, may represent palaeoseismic deformation of still plastic sediments (Shanmugam, 2017). Palaeoseismites are also reported around the Lower Chelif Basin by Guessoum et al. (2018) and interpreted as result of earthquakes of magnitude $M > 5.5$. Buchner et al. (2021) interpreted the same type of structures as a new type of seismite and a promising tool to identify strong palaeo-earthquakes.

Tectonic, sedimentological and taphonomic characteristics, as well as biotic content like those observed in the GRU deposits, have been reported from Southern Spain by Torres et al. (2022), linked to a tsunami event during the upper Pleistocene. That suggest that the event documented in our study area may be correlative to deposits observed in Southern Spain. Such correlations underline the broader regional impact of upper Pleistocene tectonics and tsunami activity in the Western Mediterranean.

6. Conclusions

The *Glycymeris*-rich Unit deposited along the coast of the Hachacha Plateau, represents a sedimentary sequence characterized by a molluscan assemblage including Senegalese fauna. These findings indicate deposition in a coastal environment ranging from the foreshore to the backshore during the upper Pleistocene, corresponding to the Last Interglacial period (MIS 5e). The GRU unconformably overlies Miocene, Pliocene, and lower Pleistocene basements. Notably, the latter is reported in this region for the first time, using a biostratigraphy approach based on nannofossils and foraminifera.

Determining the triggering mechanism of a tsunami based on the sedimentological and taphonomic characteristics of its deposits remains a challenge. We investigated all possible scenarios that could generate such events, with a particular focus on seismic activity in the study area. Our analysis used both onshore and offshore transects linked to a regional context, to better understand the interplay between tectonic processes and the resulting sedimentary evidence. The interpretation of the GRU as a tsunami-related deposit is supported by distinctive biotic, taphonomic, and sedimentological features. The biotic composition shows the presence of organisms from supralittoral to shallow circalittoral zones, along with the mixture of terrestrial and marine mollusc shells. Taphonomic evidence reveals: i) low percentages of boring and the complete absence of encrustation, combined with good to excellent shell preservation; ii) a predominance of sharp-edged shell fragmentation and a chaotic shell arrangement, with the dominance of elements oriented obliquely to vertically; iii) good shell sorting, with units dominated by shell valves within the size range of 3–5 cm; and iv) a complete lack of articulated shells. Sedimentological characteristics further support this interpretation. These include an irregular erosive base, rapid lateral facies and thickness variations, a wide range of grain sizes from sand to boulders, a mixture of rounded and angular clasts, imbrication of large blocks, normal and inverse grading within subunits, and diagnostic structures such as rip-up clasts of both soft and hard substrate, downward injections of sediment into the basement, high energy flow structures, horizontal and oblique lamination, hummocky cross-stratification (HCS), and soft sediment deformation structures (SSDS).

The presence of seismite structures beneath the GRU, associated with the tectonic context of the Hachacha Plateau, which is located in the most tectonically active zone in the Western Mediterranean, suggests that the extreme event that produced the GRU may have resulted from an offshore surface rupture of an active fault with a vertical component in the Northwestern Dahra margin or the Algerian Basin, driven by the convergence of the Eurasian and African plates.

CRediT authorship contribution statement

MAD: Writing – original draft, Conceptualization, Fieldwork, Methodology, Formal analysis, Data curation, Investigation, Visualization, Validation,

LS: Supervision, Resources, Funding acquisition, Project administration, Methodology, Fieldwork, Validation, Writing – review & editing.

CKO, LB, AHLV, HT, BL, AU, MB, MEJ, AH: Writing – review & editing.

JM: Formal analysis, Investigation, Visualization, Validation, Writing – review & editing.

SPA: Supervision, Methodology, Formal analysis, Data curation, Investigation, Visualization, Validation, Writing – review & editing.

Declaration of competing interest

The authors declare that they have no known competing financial interests or personal relationships that could have appeared to influence the work reported in this article. Given her role as Journal of Quaternary Science Reviews editor, Antje Voelker had no involvement in the peer review of this article and had no access to information regarding its peer review. Full responsibility for the editorial process for this article was delegated to another journal editor.

Acknowledgements

We thank the comments and critics by the Editor Biagio Giaccio, and by an anonymous reviewer that were helpful to clarify relevant sections of this manuscript. This study was conducted as part of the doctoral training program of the 3rd Cycle "*Geology of Marine and Continental Environments: Integrated Stratigraphy, Chronology and Dynamics of Paleoenvironments*". This work is carried out thanks to the support of the DGRSDT (General Direction of the Scientific Research and Technologic Development, Ministry of Higher Education and Scientific Research, Algeria). SPA acknowledges his former contract with project M1.1. A/INFRAEST CIENT/A/001/2021 - Base de Dados da PaleoBiodiversidade da Macaronésia, funded by the Regional Government of the Azores. SPA acknowledges his current FCT/2023.07418 CEEECIND research contract with BIOPOLIS (https://doi.org/10.54499/2023.07418.CEECIND/CP2845/CT0001. Haga clic o pulse si confía en este vínculo.">https://doi.org/10.54499/2023.07418.CEECIND/CP2845/CT0001). This work also benefitted from FEDER funds, through the Operational Program for Competitiveness Factors – COMPETE, and from National Funds, through FCT (UID/50027-Rede de Investigação em Biodiversidade e Biologia Evolutiva, POCI-01–0145-FEDER-006821, UIDB/00153/2020, LA/P/0048/2020), as well as through the Regional Government of the Azores (M1.1.a/005/Funcionamento-C-/2016, CIBIO-A; M1.1.A/INFRAEST CIENT/A/001/2021). JM acknowledges the Portuguese Fundação para a Ciência e Tecnologia, FCT, I.P./MCTES through national funds

(PIDDAC): UID/50019/2025 and LA/P/0068/2020 https://doi.org/10.54499/LA/P/0068/2020).

Data availability

All data and/or code is contained within the submission.

References

Abbouda, M., Maouche, S., Bouhadada, Y., Belhai, D., 2019. Neotectonic and active tectonics of the Dahra-lower Cheliff basin (Tell atlas, Algeria): seismotectonic implication. J. Afr. Earth Sci. 153, 250–267. https://doi.org/10.1016/j.jafrearsci.2019.02.023.

Aigner, T., 1985. Storm depositional systems. Dynamic, stratigraphy in modern and an cient shallow-marine sequences. Lect. Notes Earth Sci. 3, 174. Springer, Berlin.

Anderson, R.V., 1936. Geology in the coastal Atlas of western Algeria. Mem. Soc. Geol. Amer. 4, 486. https://doi.org/10.1130/MEM4-p1.

Ando, M., Kitamura, A., Tu, Y., Ohashi, Y., Imai, T., Nakamura, M., Ikuta, R., Miyairi, Y., Yokoyama, Y., Shishikura, M., 2018. Source of high tsunamis along the southernmost Ryukyu trench inferred from tsunami stratigraphy. Tectonophysics 722, 265–276. https://doi.org/10.1016/j.tecto.2017.11.007.

Andreucci, S., Panzeri, L., Martini, P., Maspero, F., Martini, M., Pascucci, V., 2014. Evolution and architecture of a west Mediterranean upper Pleistocene to Holocene coastal apron-fan system. Sedimentology 61, 333–361. https://doi.org/10.1111/sed.12058.

Arab, M., Bracene, R., Roure, F., Zazoun, R.S., Mahjoub, Y., Badji, R., 2015. Source rocks and related petroleum systems of the Chelif Basin, (western Tellian domain, north Algeria). Mar. Petrol. Geol. 64, 363–385. https://doi.org/10.1016/j.marpetgeo.2015.03.017.

Atif, K.F.T., Bessedik, M., Belkebir, L., Mansour, B., Saint-Martin, J.P., 2008. Le passage Mio-Pliocène dans le bassin du Bas Chélif (Algérie). Biostratigraphie et paléoenvironnements. Geodiversitas 30, 97–116.

Atik, A., Mansouri, M.E.H., Bessedik, M., Osman, M.K., Belkebir, L., Saint Martin, J.P., Chaix, C., Belkhir, A., Gorini, C., Belhadji, A., Satour, L., 2024. New insights on the latest Messinian-to-Piacenzian stratigraphic series from the Dahra massif (lower Chelif Basin, Algeria): Lago Mare, reflooding and bio-events. BSGF- Earth Sci. Bull. 195, 2. https://doi.org/10.1051/bsgf/2023012.

Ayadi, A., Maouche, S., Harbi, A., Meghraoui, M., Beldjoudi, H., Oussadou, F., Mahsas, A., Benouar, D., Heddar, A., Rouchiche, Y., Kherroubi, A., Frogneux, M., Lammali, K., Benhamouda, F., Sebaï, A., Bourouis, S., Alasset, P.J., Aoudia, A., Cakir, Z., Merahi, M., Nouar, O., Yelles, K., Bellik, A., Briole, P., Charade, O., Thouvenot, F., Semane, F., Ferkoul, A., Deramchi, A., Haned, S.A., 2003. Strong Algerian earthquake strikes near capital city. EOS. Trans Amer. Geoph. Union 84, 561. https://doi.org/10.1193/1.2720363.

Ávila, S.P., Amen, R.G., Azevedo, J., Cachão, M., García-Talavera, F., 2002. Checklist of the Pleistocene marine molluscs of Praínha and Lagoínhas (Santa Maria island, Azores). Açoreana 9, 343–370. http://hdl.handle.net/10400.3/1019.

Ávila, S.P., Madeira, P., García-Talavera, F., da Silva, C.M., Cachão, M., Martins, A.M.F., 2007. *Luria lurida* (Mollusca: Gastropoda), a new record for the Pleistocene of Santa Maria (Azores, Portugal). Arquipelago 24, 53–56.

Ávila, S.P., Madeira, P., Zazo, C., Kroh, A., Kirby, M., da Silva, C.M., Cachão, M., de Frias Martins, A.M., 2009. Palaeoecology of the Pleistocene (MIS 5.5) outcrops of Santa Maria island (Azores) in a complex oceanic tectonic setting. Palaeogeogr. Palaeoclimat., Palaeoecol. 274, 18–31. https://doi.org/10.1016/j.palaeo.2008.12.014.

Ávila, S.P., Rebelo, A.C., Medeiros, A., Melo, C., Gomes, C., Bagaço, L., Patricia, M., Borger, P.A.V., Monteiro, P., Cordriero, R., Meireles, R., Ramalho, R.P., 2010. Os fósseis de Santa Maria (Açores): 1. A jazida da Prainha. OVGA – Observatório Vulcanológico e Geotérmico dos Açores. Lagoa, p. 103. http://hdl.handle.net/10400.3/1028.

Ávila, S.P., Melo, C., Silva, L., Ramalho, R.S., Quartau, R., Hipólito, A., Cordeiro, R., Rebelo, A.C., Madeira, P., Rovere, A., Hearty, P.J., Henriques, D., Da Silva, C.M., Martins, A.M.F., Zazo, C., 2015a. A review of the MIS 5e highstand deposits from Santa Maria Island (Azores, NE Atlantic): palaeobiodiversity, palaeoecology and palaeobiogeography. Quat. Sci. Rev. 114, 126–148. https://doi.org/10.1016/j.quascirev.2015.02.012.

Ávila, S.P., Ramalho, R.S., Habermann, J.M., Quartau, R., Kroh, A., Berning, B., Jonson, M., Kirby, M.X., Zanon, V., Titshack, J., Goss, G., Rebelo, A.C., Melo, C., Madeira, P., Cordeiro, R., Meireles, R., Bagaço, L., Hipólito, A., Uchman, A., Da Silva, C.M., Cachão, M., Madeira, J., 2015b. Palaeoecology, taphonomy, and preservation of a lower Pliocene shell bed (coquina) from a volcanic oceanic island (Santa Maria Island, Azores). Palaeogeogr. Palaeoclimatol. Palaeoecol. 430, 57–73. https://doi.org/10.1016/j.palaeo.2015.04.015.

Ávila, S.P., Cachão, M., Ramalho, R.S., Botelho, A.Z., Madeira, P., Rebelo, A.C., Cordeiro, R., Melo, C., Hipólito, A., Ventura, M.A., Lipps, J.H., 2016. The palaeontological heritage of Santa Maria Island (Azores: NE Atlantic): a re-evaluation of geosites in GeoPark Azores and their use in geotourism. Geoheritage 8, 155–171. https://doi.org/10.1007/s12371-015-0148-x.

Ávila, S.P., Ramalho, R.S., Habermann, J.M., Titschack, J., 2018. The marine fossil record at Santa Maria island (Azores). In: Kueppers, U., Beier, C. (Eds.), Volcanoes of the Azores: Revealing the Geological Secrets of the Central Northern Atlantic Islands. Springer, pp. 155–196. https://doi.org/10.1007/978-3-642-32226-6_9.

Ávila, S.P., Azevedo, J.M.N., Madeira, P., Cordeiro, R., Melo, C.S., Baptista, L., Torres, P., Johnson, M.E., Vullo, R., 2020. Pliocene and late-Pleistocene actinopterygian fishes from Santa Maria island (Azores: NE Atlantic ocean): systematics, palaeoecology and palaeobiogeography. Geol. Mag. 157, 1526–1542. https://doi.org/10.1017/S0016756820000035.

Ávila, S.P., Paris, R., Ramalho, R.S., Melo, C.S., Martín-González, E., Rolán, E., Madeira, P., Ávila, G.C., Porteiro, J.M., Medeiros, A.M., Naughton, F., Abrantes, F., Martins, G.M., Johnson, M.E., Madeira, J., 2025. Mega-tsunami deposits and range expansion of cold-temperate marine species towards the tropics in glacial times. Frontiers of Biogeography 18, e138319.

Backman, J., Raffi, I., Rio, D., Fornaciari, E., Pälike, H., 2012. Biozonation and biochronology of Miocene through Pleistocene calcareous nannofossils from low and middle latitudes. Newsl. Stratigr. 45, 221–244. https://doi.org/10.1127/0078-0421/2012/0022.

Badji, R., Charvis, P., Bracene, R., Galve, A., Badsi, M., Ribodetti, A., Benaissa, Z., Klingelhoefer, F., Medaouri, M., Beslier, M.O., 2015. Geophysical evidence for a transform margin offshore Western Algeria: a witness of a subduction-transform edge propagator? Geoph. J. Intell. 200, 1027–1043. https://doi.org/10.1093/gji/ggu454.

Barbano, M.S., Pirrotta, C., Gerardi, F., 2010. Large boulders along the south-eastern Ionian coast of Sicily: storm or tsunami deposits? Mar. Geol. 275, 140–154. https://doi.org/10.1016/j.margeo.2010.05.005.

Barclay, K.M., Gingras, M.K., Packer, S.T., Leighton, L.R., 2020. The role of gastropod shell composition and microstructure in resisting dissolution caused by ocean acidification. Mar. Environ. Res. 162, 105105. https://doi.org/10.1016/j.marenvres.2020.105105.

Bard, E., Cornu, S., Pätzold, J., 1994. Temperature of the last interglacial based on $\delta^{18}O$ in Mollusks. In: Long-Term Climatic Variations: Data and Modelling. Springer, Berlin, Heidelberg, Berlin Heidelberg, pp. 259–266. https://doi.org/10.1007/978-3-642-79066-9_11.

Bardají, T., Goy, J.L., Zazo, C., Hillaire-Marcel, C., Dabrio, C.J., Cabero, A., Ghaleb, B., Silva, P.G., Lario, J., 2009a. Sea level and climate changes during OIS 5e in the Western Mediterranean. Geomorphology 104, 22–37. https://doi.org/10.1016/j.geomorph.2008.05.027.

Bardají, T., Goy, J.L., Zazo, C., Hillaire-Marcel, C., Dabrio, C.J., Cabero, A., Ghaleb, B., Silva, P.G., Lario, J., 2009b. Reply to the comments by Mauz, B. and Antonioli, F. on "Sea Level and Climate Changes during OIS 5e in the Western Mediterranean". Geomorphology 110, 231–235. https://doi.org/10.1016/j.geomorph.2009.05.007.

Benjamin, J., Rovere, A., Fontana, A., Furlani, S., Vacchi, M., Inglis, R.H., Galili, E., Antonioli, F., Sivan, D., Miko, S., Mourtzas, N., Felja, I., Meredith-Williams, M., Goodman Tchernov, B., Kolaiti, E., Anzidei, M., Gehrels, R., 2017. Late Quaternary sea-level changes and early human societies in the central and eastern Mediterranean Basin: an interdisciplinary review. Quat. Int. 449, 29–57. https://doi.org/10.1016/j.quaint.2017.06.025.

Belhadji, A., Belkebir, L., Saint Martin, J.P., Mansour, B., Bessedik, M., Conesa, G., 2008. Apports des foraminifères planctoniques à la biostratigraphie du Miocène supérieur et du Pliocène de Djebel Diss (bassin du Chélif, Algérie). Geodiversitas 30, 79–96. http://sciencepress.mnhn.fr/fr/periodiques/geodiversitas/30/1/.

Belkebir, L., Anglada, R., 1985. Le Néogène de la bordure nord occidentale du massif du Dahra. In: 110è Congr. Natl. Soc. Savantes, Sciences 6, pp. 279–290. Montpellier. https://cths.fr/ed/edition.php?id=156.

Belkebir, L., 1986. Le Néogène de la bordure nord occidentale du massif de Dahra (Algérie). Biostratigraphie, paléoécologie, paléogéographie. PhD Thesis. Provence University, p. 289 (unpublished).

Belkebir, L., Bessedik, M., Ameur-Chehbeur, A., Anglada, R., 1996. Le Miocène des bassins nord-occidentaux d'Algérie : biostratigraphie et eustatisme. Elf Aquitaine. Paunch 16, 553–561.

Belkebir, L., Bessedik, M., Mansour, B., 2002. Le Miocène supérieur du bassin du Bas Chélif: attribution biostratigraphique à partir des foraminifères planctoniques. Mem. Serv. Geol. Algerie 11, 187–194.

Belkebir, L., Labdi, A., Mansour, B., Bessedik, M., Saint Martin, J.P., 2008. Biostratigraphie et lithologie des séries serravallo-tortoniennes du massif du Dahra et du bassin du Chélif (Algérie). Implications sur la position de la limite serravallo-tortonienne. Geodiversitas 30, 9–19.

Benyoucef, M., Bendella, M., Brunettic, M., Ferréd, B., Kocie, T., Bouchemla, I., Slamif, R., Ghenimg, A.F., 2021. Upper Pliocene bivalve shell concentrations from the Lower Chelif basin (NW Algeria): systematics, sedimentologic and taphonomic framework. Ann. Paleontol. 107, 102509. https://doi.org/10.1016/j.annpal.2021.1025090753-3969.

Benyoucef, M., Landau, B., 2025. Systematics and taphonomy of Pliocene Gastropoda (Mollusca) from the Dahra Mountains, NW Algeria. Ann. Paleontol. 111, 1–21. https://doi.org/10.1016/j.annpal.2024.102752, 102752.

Bessedik, M., Belkebir, L., Mansour, B., 2002. Révision de l'âge miocène inférieur (au sens des anciens auteurs) des dépôts du Bassin du Bas Chélif (Oran, Algérie) : conséquences biostratigraphique et géodynamique. Mém. d Serv. Géol. Algér. 11, 167–186.

Billi, A., Cuffaro, M., Orecchio, B., Palano, M., Presti, D., Totaro, C., 2023. Retracing the Africa – Eurasia nascent convergent boundary in the Western Mediterranean based on earthquake and GNSS data. Earth Planet Sci. Lett. 601, 117906. https://doi.org/10.1016/j.epsl.2022.117906.

Bown, P.R., Young, J.R., 1998. Techniques. In: Bown, P.R. (Ed.), Calcareous Nannofossil Biostratigraphy. Kluwer Academic Publ., Dordrecht, the Netherlands, pp. 16–28.

Brill, D., May, S.M., Mhammdi, N., King, G., Brückner, H., 2017. OSL surface exposure dating of wave-emplaced coastal boulders – research concept and first results from the Rabat coast, Morocco. Geophys. Res. Abstr. 19, EGU2017–12947.

Buchner, E., Sach, V.J., Schmieder, M., 2021. Sand spikes pinpoint powerful palaeoseismicity. Nat. Commun. 12, 6731. https://doi.org/10.1038/s41467-021-27061-6.
Cerrone, C., Vacchi, M., Fontana, A., Rovere, A., 2021. Last Interglacial sea-level proxies in the western Mediterranean. Earth Syst. Sci. Data 13, 4485–4527. https://doi.org/10.5194/essd-13-4485-2021.
Chakroun, A., Zaghbib-Turki, D., 2017. Facies and fauna proxies used to reconstruct the MIS 5 and MIS 7 coastal environments in eastern Tunisia. Geol. Quat. 61 (2). https://doi.org/10.7306/gq.1312.
Cornu, S., Pätzold, J., Bard, E., Meco, J., Cuerda-Barcelo, J., 1993. Paleotemperature of the last interglacial period based on $\delta^{18}O$ of *Strombus bubonius* from the western Mediterranean Sea. Palaeogeogr. Palaeoclimatol. Palaeoecol. 103, 1–20. https://doi.org/10.1016/0031-0182(93)90047-M.
Dalloni, M., 1953. La limite du Tertiaire et du Quaternaire dans le nord-ouest de l'Algérie et des contrées voisines. 4th INQUA congress 1, 19–29. Pisa.
Dattilo, B.F., Brett, C.E., Tsujita, C.J., Fairhurst, R., 2008. Sediment supply versus storm winnowing in the development of muddy and shelly interbeds from the Upper Ordovician of the Cincinnati region, USA. Can. J. Earth Sci. 45, 243–265. https://doi.org/10.1139/E07-060.
Davies, D.J., Powell, E.N., Stanton, R.J.Jr, 1989. Taphonomic signature as a function of environmental process: shells and shell beds in a hurricane-influenced inlet on the Texas coast. Palaeogeogr. Palaeoclimatol. Palaeoecol. 72, 317–356. https://doi.org/10.1016/0031-0182(89)90150-8.
Dawson, A.G., Stewart, I., 2007. Tsunami deposits in the geological record. Sed. Geol. 200, 166–183. https://doi.org/10.1016/j.sedgeo.2007.01.002.
de Lamothe, G., 1911. Anciennes lignes de rivage du Sahel d'Alger. Mém. soc. Géol. Fr 6, 288.
Delfaud, J., Michaux, J., Neurdin, J., Revert, J., 1973. Un modèle paléogéographique de la bordure méditerranéenne : évolution de la région oranaise (Algérie) au Miocène supérieur. Conséquences stratigraphiques. Bull. Soc. Hist. Nat. Afr. Nord Alger 64, 219–241.
Delteil, J., 1974. Tectonique de la chaine alpine en Algérie d'après l'étude du Tell oranais (Monts de la Mina, Beni Chougrane, Dahra). Thèse Doctorat Sci., Nice University.
del Valle, L., Timar-Gabor, A., Fornós, J.J., 2024. Chronology of Pleistocene sedimentary cycles in the western Mediterranean. Quat. Sci. Rev. 330, 108451. https://doi.org/10.1016/j.quascirev.2023.108451.
DeMets, C., Gordon, R.G., Argus, D.F., Stein, S., 1990. Current plate motions. Geoph. J. Intell. 101, 425–478. https://doi.org/10.1111/j.1365-246X.1990.tb06579.x.
DeMets, C., Gordon, R.G., Argus, D.F., 2010. Geologically current plate motions. Geophys. J. Int. 181, 1–80. https://doi.org/10.1111/j.1365-246X.2009.04491.x.
Domzig, A., Yelles, K., Le Roy, C., Déverchère, J., Bouillin, J.P., Bracene, R., Mercier de Lepinay, B., Le Roy, P., Calais, E., Kherroubi, K., Gaullier, V., Savoye, B., Pauc, H., 2006. Searching for the Africa-Eurasia Miocene boundary onshore western Algeria (Maradja'03 cruise). C. R. Geosci. 338, 80–91. https://doi.org/10.1016/j.crte.2005.11.009.
Donato, S.V., Reinhardt, E.G., Boyce, J.I., Rothaus, R., Vosmer, T., 2008. Identifying tsunami deposits using bivalve shell taphonomy. Geology 36, 199–202. https://doi.org/10.1130/G24554A.1.
Donato, S.V., Reinhardt, E.G., Boyce, J.I., Pilarczyk, J.E., Jupp, B.P., 2009. Particle-size distribution of inferred tsunami deposits in Sur Lagoon, Sultanate of Oman. Mar. Geol. 257, 54–64. https://doi.org/10.1016/j.margeo.2008.10.012.
Doumergue, F., 1922. Description de deux stations préhistoriques à quartzites taillés des environs de Karouba (Mostaganem) et considérations sur leurs relations stratigraphiques avec la plage émergée du niveau de 18 mètres. Bull. Soc. Géogr. Archéol. Prov. Oran 42 (162), 42.
Duquette, A., McClintock, J.B., Amsler, C.D., Pérez-Huerta, A., Milazzo, M., Hall-Spencer, J.M., 2017. Effects of ocean acidification on the shells of four Mediterranean gastropod species near a CO_2 seep. Mar. Pollut. Bull. 124, 917–928. https://doi.org/10.1016/j.marpolbul.2017.08.007.
Engel, M., Brückner, H., 2011. The identification of palaeo-tsunami deposits– a major challenge in coastal sedimentary research. Coast. Res. 17, 65–80.
Engel, M., Oetjen, J., May, S.M., Brückner, H., 2016. Tsunami deposits of the Caribbean towards an improved coastal hazard assessment. Earth Sci. Rev. 163, 260–296. https://doi.org/10.1016/j.earscirev.2016.10.010.
Freneix, S., Saint Martin, J.P., Moissette, P., 1987a. Bivalves Ptériomorphes du Messinien d'Oranie (Algérie occidentale). Bul. Mus. Nat. Hist. Nat., 4ème sér. 9, 3–61. Sect. C (1).
Freneix, S., Saint Martin, J.P., Moissette, P., 1987b. Bivalve Hétérodontes du Messinien d'Oranie (Algérie occidentale). Bul. Mus. Nat. Hist. Nat., 4ème sér. 9, 415–453. Sect. C (4).
Freneix, S., Saint Martin, J.P., Moissette, P., 1988. Huîtres du Messinien d'Oranie (Algérie occidentale) et Paléo biologique de l'ensemble de la faune de bivalves). Bul. Mus. Nat. Hist. Nat., 4ème sér. 10, 1–21. Sect. C (1).
Fujiwara, O., Kamataki, T., Fuse, K., 2003. Genesis of mixed molluscan assemblages in the tsunami deposits distributed in Holocene drowned valleys on the southern Kanto region, east Japan. Quat. Res. (Daiyonki-Kenkyu) 42, 389–412. https://doi.org/10.4116/jaqua.42.389 (in Japanese with English abstract).
Fujiwara, O., Kamataki, T., 2007. Identification of tsunami deposits considering the tsunami waveform: an example of subaqueous tsunami deposits in Holocene shallow bay on southern Boso Peninsula, Central Japan. Sed. Geol. 200, 295–313. https://doi.org/10.1016/j.sedgeo.2007.01.009.
Gartner, S., 1977. Calcareous nannofossil biostratigraphy and revised zonation of the Pleistocene. Mar. Micropaleont 2, 1–25. https://doi.org/10.1016/0377-8398(77)90002-0.
Gelfenbaum, G., Jaffe, B., 2003. Erosion and sedimentation from the 17 July, 1998 Papua New Guinea tsunami. Pure Appl. Geophys. 160, 1969–1999. https://doi.org/10.1007/s00024-003-2416-y.
Gerber, J., Hemmen, J., Groh, K., 1989. Eine pleistozäne marine Molluskenfauna von Porto Santo (Madeira-Archipel). Mitt. Dtsch. Malakozool. Ges. 44–45, 19–30.
Gignoux, M., 1911. Les couches à *Strombus bubonius* (LMK) dans la Méditerranée occidentale. C. R. Acad. Sci. 15, 339. Paris.
Glangeaud, L., 1932. Etude géologique de la région Littorale de la province d'Alger. Thèse Sci. Paris et bull. Serv. Carte Géol. Alger. 2ème sér 8.
Goff, J.R., McFadgen, B.G., Chague-Goff, C., 2004. Sedimentary differences between the 2002 Easter storm and the 15th century Okoropunga tsunami, southeastern North Island, New Zealand. Mar. Geol. 204, 235–250. https://doi.org/10.1016/S0025-3227(03)00352-9.
Goto, K., Chavanich, S.A., Imamura, F., Kunthasap, P., Matsui, T., Minoura, K., Sugawara, D., Ynagisawa, H., 2007. Distribution, origine and transport process of boulders deposited by the 2004 Indian Ocean tsunami at Pakargang Cape, Thailand. Sed. Geol. 202, 821–837. https://doi.org/10.1016/j.sedgeo.2007.09.004.
Gourinard, Y., 1958. Recherches sur la géologie du littoral Oranais. Pub. Serv. Carte Géol. Algérie, série A 2809. Alger.
Guardia, P., 1975. Géodynamique de la marge alpine du continent africain d'après l'étude de l'Oranie nord-occidentale. PhD thesis, Nice University.
Guessoum, N., Benhamouche, A.A., Bouhadad, Y., Bourenane, H., Abbouda, M., 2018. Field evidence of Quaternary seismites in the Mostaganem-Relizane (western Algeria) region: seismotectonic implication. Arabian J. Geosci. 11 (20), 641. https://doi.org/10.1007/s12517-018-4009-1.
Gutiérrez-Mas, J.M., Juan, C., Morales, J.A., 2009. Evidence of high-energy events in shelly layers interbedded in coastal Holocene sands in Cadiz Bay (south-west Spain). Earth Surf. Process. Landf. 34, 810–823. https://doi.org/10.1002/esp.1770.
Harzhauser, M., Kronenberg, G.C., 2013. The Neogene strombid gastropod *Persististrombus* in the Paratethys sea. Acta Palaeontol. Pol. 58, 785–802. https://doi.org/10.4202/app.2011.0130.
Hori, K., Kuzumoto, R., Hirouchi, D., Umitsu, M., Janjirawuttikul, N., Patanakanog, B., 2007. Horizontal and vertical variation of 2004 Indian tsunami deposits: an example of two transects along the western coast of Thailand. Mar. Geol. 239, 163–172. https://doi.org/10.1016/j.margeo.2007.01.005.
Hyžný, M., Melo, C.S., Ramalho, R.S., Cordeiro, R., Madeira, P., Baptista, L., Rebelo, A.C., Gómez, C., Torres, P., Uchman, A., Johnson, M.E., Berning, B., Ávila, S.P., 2021. Pliocene and Late Pleistocene (MIS 5e) decapod crustacean crabs from Santa Maria Island (Azores Archipelago: NE Atlantic): systematics, palaeoecology and palaeobiogeography. J. Quat. Sci. 36, 91–109. https://doi.org/10.1002/jqs.3261.
Khadraoui, A., Kamoun, M., Hamad, A.B., Zaïbi, C., Bonnin, J., Viehberg, F., Bahrouni, N., Sghari, A., Abida, H., Kamoun, F., 2018. New insights from microfauna associations characterizing palaeoenvironments, sea level fluctuations and a tsunami event along Sfax Northern coast (Gulf of Gabes, Tunisia) during the Late Pleistocene-Holocene. J. Afr. Earth Sci. 147, 411–429. https://doi.org/10.1016/j.jafrearsci.2018.05.011.
Kidwell, S.M., Fürsich, F.T., Aigner, T., 1986. Conceptual framework of the analysis and classification of fossil concentrations. Palaios 1, 228–238. https://doi.org/10.2307/3514687.
Kidwell, S.M., Holland, S.M., 1991. Field description of coarse bioclastic fabrics. Palaios 6, 426–434.
King, G.C.P., Vita-Finzi, C., 1981. Active folding in the Algerian earthquake of 10 October 1980. Nature 292 (5818), 22–26. https://doi.org/10.1038/292022a0.
Kitamura, A., Ito, M., Ikuta, R., Ikeda, M., 2018. Using molluscan assemblages from paleotsunami deposits to evaluate the influence of topography on the magnitude of late Holocene mega-tsunamis on Ishigaki Island, Japan. Prog. Earth Planet. Sci. 5, 41. https://doi.org/10.1186/s40645-018-0200-y.
Kreipl, K., Poppe, G.T., 1999. A Conchological Iconography – the Family Strombidae. ConchBooks (formerly Christa Hemmen, Hackenheim, pp. 1–58.
Laffitte, R., 1950. Sur l'existence du Calabrien dans la région oranaise. C. R. Acad. Sci. 230, 217–219. Paris.
Leprêtre, R., De Lamotte, D.F., Combier, V., Gimeno-Vives, O., Mohn, G., Eschard, R., 2018. The Tell-Rif orogenic system (Morocco, Algeria, Tunisia) and the structural heritage of the southern Tethys margin. BSGF Earth Sci. Bull. 189, 1–35. https://doi.org/10.1051/bsgf/2018009.
Lirer, F., Foresi, L.M., Iaccarino, S.M., Salvatorini, G., Turco, E., Cosentino, C., 2019. Mediterranean Neogene planktonic foraminifer biozonation and biochronology. Earth Sci. Rev. 196 (102869), 1–36. https://doi.org/10.1016/j.earscirev.2019.05.013.
Lofi, J., Sage, F., Déverchère, J., Loncke, L., Maillard, A., Gaullier, V., Thinon, I., Gillet, H., Guennoc, P., Gorini, C., 2011. Refining our knowledge of the Messinian salinity crisis records in the offshore domain through multi-site seismic analysis. Bull. Soc. Geol. Fr. 182, 163–180. https://doi.org/10.2113/gssgfbull.182.2.163.
Lourens, L.J., Sluijs, A., Kroon, D., Zachos, J.C., Thomas, E., Röhl, U., Bowles, J., Raffi, I., 2005. Astronomical pacing of late Palaeocene to early Eocene global warming events. Nature 435 (7045), 1083–1087. https://doi.org/10.1038/nature03814.
Madeira, J., Ramalho, R.S., Hoffmann, D.L., Mata, J., Moreira, M., 2020. A geological record of multiple Pleistocene tsunami inundations in an oceanic island: the case of Maio, Cape Verde. Sedimentology 67, 1529–1552. https://doi.org/10.1111/sed.12612.
Madeira, P., Kroh, A., Martins, A.M.F., Ávila, S.P., 2007. The marine fossils from Santa Maria Island (Azores, Portugal): an historical overview. Açoreana, Supl. 5, 59–73.
Mansouri, M.E.H., Bessedik, M., Aubbry, M.P., Belkebir, L., Mansour, B., Beaufort, L., 2008. Contribution biostratigraphiques et paléo environnementales de l'étude des nannofossiles calcaires des dépôts tortono-messiniens du bassin du Chélif (Algérie).

Geodiversitas 30, 59–77. http://sciencepress.mnhn.fr/fr/periodiques/geodiversitas/30/1/.
Maouche, S., Morhange, C., Meghraoui, M., 2009. Large boulder accumulation on the Algerian coast evidence tsunami events in the western Mediterranean. Mar. Geol. 262, 96–104. https://doi.org/10.1016/j.margeo.2009.03.013.
Maouche, S., Bouhadad, Y., Harbi, A., Rouchiche, Y., Ousadou, F., Ayadi, A., 2019. Active tectonics and seismic hazard in the Tell Atlas (Northern Algeria): a review. The Geology of the Arab World – An Overview 381–400. https://doi.org/10.1007/978-3-319-96794-3_10.
Martín-González, E., Galindo, I., Mangas, J., Romero, C., Sánchez, N., González-Rodríguez, A., Coello Bravo, J.J., Márquez, A., De Vera, A., Vegas, J., Melo, C.S., 2019. Revisión de los depósitos costeros del estadio isotópico marino 5e (MIS 5e) de Fuerteventura (islas Canarias). Vieraea 46, 667–688. https://doi.org/10.31939/vieraea.2019.46.tomo02.12.
Massari, F., D'Alessandro, A., Davaud, E., 2009. A coquinoid tsunamite from the Pliocene of Salento (SE Italy). Sediment. Geol. 221, 7–18. https://doi.org/10.1016/j.sedgeo.2009.07.007.
Matougui, R., Haddoum, H., 2008. Mise en évidence de mouvements gravitaires sur la pente continentale de la marge du Dahra occidental (Ténès – Cap Ivi). Bull. Serv. Géol. National 19, 267–285.
Matsumoto, D., Shimamoto, T., Hirose, T., Gunatilake, J., Wickramasooriya, A., DeLile, J., Young, S., Rathnayake, C., Ranasooriya, J., Murayama, M., 2010. Thickness and grain-size distribution of the 2004 Indian Ocean tsunami deposits in Periya Kalapuwa Lagoon, eastern Sri Lanka. Sediment. Geol. 230, 95–104. https://doi.org/10.1016/j.sedgeo.2010.06.021.
Marriner, N., Kaniewski, D., Morhange, C., Flaux, C., Giaime, M., Vacchi, M., Goff, J., 2017. Tsunamis in the geological record: making waves with a cautionary tale from the Mediterranean. Sci. Adv. 3, 1–12. https://doi.org/10.1126/sciadv.1700585.
Mauz, B., Hassler, U., 2000. Luminescence chronology of Late Pleistocene raised beaches in southern Italy: new data of relative sea-level changes. Mar. Geol. 170, 187–203. https://doi.org/10.1016/S0025-3227(00)00074-8.
Mauz, B., Elmejdoub, N., Nathan, R., Jedoui, Y., 2009. Last interglacial coastal environments in the Mediterranean–Saharan transition zone. Palaeogeogr. Palaeoclimat., Palaeoecol. 279, 137–146. https://doi.org/10.1016/j.palaeo.2009.05.006.
Mauz, B., Antonioli, F., 2009. Comment on "Sea level and climate changes during MIS 5e in the Western Mediterranean" by T. Bardají, JL Goy, JL, C. Zazo, C. Hillaire-Marcel, CJ Dabrio, A. Cabero, B. Ghaleb, PG Silva, J. Lario, Geomorphology 104 (2009), 22–37. Geomorphology 110, 227–230. https://doi.org/10.1016/j.geomorph.2009.05.001.
Mazzola, G., 1971. Les foraminifères planctoniques du Mio-Pliocène de l'Algérie nord-occidentale. In: Program II Planktonic Conference. A. Farrinacci, pp. 787–812. Roma.
Meco, J., 1977. Los *Strombus* neógenos y cuaternarios del Atlántico euroafricano. Taxonomía, biostratigrafia y paleoecología. Ediciones Cabildo de Gran Canaria, Madrid 207.
Meco, J., Petit-Maire, N., Fontugne, M., Shimmield, G., Ramos, A.J., 1997. The Quaternary deposits in Lanzarote and Fuerteventura (eastern canary Islands, Spain): an overview. In: Meco, J., Petit-Maire, N. (Eds.), Proceedings of the Climates of the Past Meeting, June 2–7, 1995 Lanzarote and Fuerteventura (Canary Islands, Spain). Universidad de Las Palmas de Gran Canaria, pp. 123–136.
Meco, J., Guillou, H., Carracedo, J.C., Lomoschitz, A., Ramos, A.J.G., Rodríguez-Yánez, J.J., 2002. The maximum warmings of the Pleistocene world climate recorded in the Canary Islands. Palaeogeogr. Palaeoclimatol. Palaeoecol. 185, 197–210. https://doi.org/10.1016/S0031-0182(02)00300-0.
Meghraoui, M., 1982. Etude néotectonique de la région nord-est d'El Asnam: relation avec le séisme du 10 octobre 1980. PhD thesis. Paris XII University.
Meghraoui, M., Philip, H., Albarède, F., Cisternas, A., 1988. Trenches investigations through the trace of the 1980 El-Asnam thrust fault: evidence for paleoseismicity. Bull. Seismol. Soc. Am. 78, 979–999. https://doi.org/10.1785/BSSA0780020979.
Meghraoui, M., Morel, J., Andrieux, J., Dahmani, M., 1996. Tectonique plio-quaternaire de la chaine tello-rifaine et de la mer d'Alboran. Une zone complexe de convergence continent-continent. Bull. Soc. Geol. Fr. 167, 141–157.
Meghraoui, M., Maouche, S., Chemaa, B., Cakir, Z., Aoudia, A., Harbi, A., Alasset, P.-J., Ayadi, A., Bouhadad, Y., Benhamouda, F., 2004. Coastal uplift and thrust faulting as sociated with the Mw = 6.8 Zemmouri (Algeria) earthquake of 21 May, 2003. Geophys. Res. Lett. 31, L19605. https://doi.org/10.1029/2004GL020466.
Melo, C.S., Martín-González, E., Da Silva, C.M., Galindo, I., González-Rodríguez, A., Baptista, L., Rebelo, A.C., Madeira, P., Voelker, A.H.L., Johnson, M.E., Arruda, S.A., Ávila, S.P., 2022a. Range expansion of tropical shallow-water marine molluscs in the NE Atlantic during the last interglacial (MIS 5e): Causes, consequences and utility of ecostratigraphic indicators for the Macaronesian archipelagos. Quat. Sci. Rev. 278, 107377. https://doi.org/10.1016/j.quascirev.2022.107377.
Melo, C.S., Martín-González, E., Da Silva, C.M., Galindo, I., González-Rodríguez, A., Baptista, L., Rebelo, A.C., Madeira, P., Voelker, A.H.L., Johnson, M.E., Arruda, S.A., Ávila, S.P., 2022b. Reply to the comment by Meco et al. on "Range expansion of tropical shallow-water marine molluscs in the NE Atlantic during the last interglacial (MIS 5e): Causes, consequences and utility of ecostratigraphic indicators for the Macaronesian archipelagos". Quat. Sci. Rev. 288, 107535. https://doi.org/10.1016/j.quascirev.2022.107535.
Melo, C.S., Da Silva, C.M., Scarponi, D., González, E., Rolán, E., Rojas, A., Martinez, S., Silva, L., Johnson, M.E., Rebelo, A.C., Baptista, L., Voelker, A., Ramalho, R., Ávila, S. P., 2023. Palaeobiogeography of NE Atlantic archipelagos during the Last Interglacial (MIS 5e): A molluscan approach to the conundrum of Macaronesia as a marine biogeographic unit. Quat. Sci. Rev. 319, 108313. https://doi.org/10.1016/j.quascirev.2023.108313.
Morales, J.A., Borrego, J., San Miguel, E.G., López-González, N., Carro, B., 2008. Sedimentary record of recent tsunamis in the Huelva Estuary (southwestern Spain). Quat. Sci. Rev. 27, 734–746. https://doi.org/10.1016/j.quascirev.2007.12.002.
Morton, R.A., Gelfenbaum, G., Jaffe, B.E., 2007. Physical criteria for distinguishing sandy tsunami and storm deposits using modern examples. Sediment. Geol. 200, 184–207. https://doi.org/10.1016/j.sedgeo.2007.01.003.
Muhs, D.R., Meco, J., Simmons, K.R., 2014. Uranium-series ages of corals, sea level history, and palaeozoogeography, Canary Islands, Spain: an exploratory study for two Quaternary interglacial periods. Palaeogeogr. Palaeoclimatol. Palaeoecol. 394, 99–118. https://doi.org/10.1016/j.palaeo.2013.11.015.
Naimi, M.N., Cherif, A., Mahboubi, C.Y., Bachagha Bensaci, M., Mazouzi, A., Benkhedda, A., Laouini, H., 2023. Palaeoecological, taphonomic and biosedimentary analysis of Mid-Holocene lacustrine deposits from Ouargla area (Lower Sahara, SE Algeria). N. Jb. Geol. Paläont. Abh. 307, 65–80. https://doi.org/10.1127/njgpa/2023/1113.
Neurdin-Trescartes, J., 1992. Le remplissage sédimentaire du bassin néogène du Chélif, modèle de référence de bassins intramontagneux, 1. Pau & Pays de l'Adour University, p. 332. PhD thesis.
Neurdin-Trescartes, J., 1995. Paléogéographie du Bassin du Chélif (Algérie) au Miocène. Causes et conséquences. Géol. Mediterranea 22, 61–71.
Nishimura, Y., Miyaji, N., 1995. Tsunami deposits from the 1993 Southwest Hokkaido earthquake and the 1640 Hokkaido Komagatake Eruption, northern Japan. Pure Appl. Geophys. 144, 719–733.
Nocquet, J.M., Calais, E., 2004. Geodetic measurements of crustal deformation in the western Mediterranean and Europe. Pure Appl. Geophys. 161, 661–681. https://doi.org/10.1007/s00024-003-2468-z.
Osman, M.K., Bessedik, M., Belkebir, L., Mansouri, M.E.H., Atik, A., Belkhir, A., Rubino, J.L., Satour, L., Belhadji, A., 2021. Messinian to Piacenzian deposits, erosion, and subsequent marine bioevents in the Dahra massif (lower Chelif Basin, Algeria). Arabian J. Geosci. 14, 1–36. https://doi.org/10.1007/s12517-021-06481-0.
Ouyed, M., Meghraoui, M., Cisternas, A., Deschamp, A., Dorel, J., Frechet, F., Gaulon, R., Hatzfeld, D., Philip, H., 1981. Seismotectonics of the El Asnam earthquake. Nature 292 (5818), 26–31. https://doi.org/10.1038/292026a0.
Paris, R., Giachetti, T., Chevalier, J., Guillou, H., Frank, N., 2011. Tsunami deposits in Santiago Island (Cape Verde archipelago) as possible evidence of a massive flank failure of Fogos volcano. Sediment. Geol. 239, 129–145. https://doi.org/10.1016/j.sedgeo.2011.06.006.
Paris, R., Ramalho, R.S., Madeira, J., Ávila, S.P., May, S.M., Rixhon, G., Engel, M., Brückner, H., Herzog, M., Schukraft, G., Pérez-Torrado, F.J., Rodriguez-Gonzalez, A., Carracedo, J.C., Giachetti, T., 2018. Mega-tsunami conglomerates and flank collapses of ocean island volcanoes. Mar. Geol. 395, 168–187. https://doi.org/10.1016/j.margeo.2017.10.004.
Perrodon, A., 1957. Étude géologique des bassins néogènes sub-littoraux de l'Algérie occidentale. Bull. Serv. Carte Géol.Algér. 12, 1–382.
Philip, H., Meghraoui, M., 1983. Structural analysis and interpretation of the surface deformations of the El Asnam earthquake of October 10, 1980. Tectonics 2, 17–49. https://doi.org/10.1029/TC002i001p00017.
Puga-Bernabéu, Á., Martín, J.M., Braga, J.C., 2007. Tsunami-related deposits in temperate carbonate ramps, Sorbas Basin, southern Spain. Sediment. Geol. 199, 107–127. https://doi.org/10.1016/j.sedgeo.2007.01.020.
Puga-Bernabéu, A., Aguirre, J., 2017. Contrasting storm-versus tsunami-related shell beds in shallow-water ramps. Palaeogeogr. Palaeoclimatol. Palaeoecol. 471, 1–14. https://doi.org/10.1016/j.palaeo.2017.01.033.
Raffi, I., Backman, J., Rio, D., Shackleton, N.J., 1993. Plio-pleistocene nannofossil biostratigraphy and calibration to oxygen isotope stratigraphies from deep sea Drilling project site 607 and ocean Drilling program site 677. Paleoceanography 8, 387–408. https://doi.org/10.1029/93PA00755.
Raffi, I., Backman, J., Fornaciari, E., Pälike, H., Rio, D., Lourens, L., Hilgen, F., 2006. A review of calcareous nannofossil astrobiochronology encompassing the past 25 million years. Quat. Sci. Rev. 25, 3113–3137. https://doi.org/10.1016/j.quascirev.2006.07.007.
Ramalho, R.S., Winckler, G., Madeira, J., Helffrich, G.R., Hipólito, A.R., Quartau, R., Adena, K., Schaefer, J.M., 2015. Hazard potential of volcanic flank collapses raised by new megatsunami evidence. Sci. Adv. 1, e1500456. https://doi.org/10.1126/sciadv.1500456.
Ramirez, R., Tuya, F., Haroun, R.J., 2009. Spatial patterns in the population structure of the whelk *Stramonita haemastoma* (Linnaeus, 1766) (Gastropoda: Muricidae) in the Canarian archipelago (eastern Atlantic). Sci. Mar. 73, 431–437. https://doi.org/10.3989/scimar.2009.73n3431.
Ramírez-Herrera, M.T., Lagos, M., Hutchinson, I., Kostoglodov, V., Machain, M.L., Caballero, M., Goguitchaivili, A., Aguilar, B., Chagué-Goff, C., Goff, J., Ruiz-Fernández, A.C., Ortiz, M., Nava, H., Bautista, F., I.Lopez, G., Quintana, P., 2012. Extreme wave deposits on the Pacific coast of Mexico: tsunamis or storms? — a multi-proxy approach. Geomorphology 139, 360–371. https://doi.org/10.1016/j.geomorph.2011.11.002.
Reinhardt, E.G., Pilarczyk, J., Brown, Al, 2012. Probable tsunami origin for a shell and sand sheet from marine ponds on Anegada, British Virgin Islands. Nat. Hazards 63, 101–117. https://doi.org/10.1007/s11069-011-9730-y.
Rio, D., 1982. The fossil distribution of coccolithophore genus Gephyrocapsa Kamptner and related Plio–Pleistocene chronostratigraphic problems. In: Initial Report of the Deep Sea Drilling Project. US Govt Printing Office; UK Distributors, IPOD Committee, pp. 325–343. https://doi.org/10.2973/dsdq.proc.68.109.1982. NERC, Swindon.
Rodrigues, M.G., Giovanini Varejão, F., Fürsich, F.T., Christofoletti, B., Matos, S.A., Warren, L.V., Inglez, L., Cerri, R.I., Assine, M.L., Simões, M.G., 2024. Not all shell

beds are made equal: Recognizing singular event-concentrations in megalakes. Sedimentology 71, 4–47. https://doi.org/10.1111/sed.13221.
Roig-Munar, F.X., Gelabert, B., Rodríguez-Perea, A., Martín-Prieto, J.Á., Vilaplana, J.M., 2023. Storm or tsunamis: boulder deposits on the rocky coasts of the Balearic Islands (Spain). Mar. Geol. 463, 107112. https://doi.org/10.1016/j.margeo.2023.107112.
Rossetti, D.D.F., Góes, A.M., Truckenbrodt, W., Anaisse, J., 2000. Tsunami-induced large-scale scour-and-fill structures in Late Albian to Cenomanian deposits of the Grajaú Basin, northern Brazil. Sedimentology 47, 309–323. https://doi.org/10.1046/j.1365-3091.2000.00292.x.
Rouchy, J.M., Caruso, A., Pierre, C., Blanc-Valleron, M.M., Bassetti, M.A., 2007. The end of the Messinian salinity crisis: evidences from the Chelif basin (Algeria). Paleogeogr. Paleoclimat. Paleoecol. 254, 386–417. https://doi.org/10.1016/j.palaeo.2007.06.015.
Roure, F., Casero, P., Addoum, B., 2012. Alpine inversion of the North African Margin, and delamination of its continental crust. Tectonics 31, TC3006. https://doi.org/10.1029/2011TC002989.
Satour, L., Lauriat-Rage, A., Belkebir, L., Saint Martin, J.P., Mansour, B., Bessedik, M., 2011. Les bivalves ptériomorphes du Tortonien supérieur du Dahra : systématique et paléoécologie. Bull. Service géol. Nat 22, 119–139.
Satour, L., Lauriat-Rage, A., Belkebir, L., Bessedik, M., 2013. Biodiversity and taphonomy of bivalves assemblages of the Pliocene of Algeria (Bas Chelif basin). Arabian J. Geosci. 7, 1–14. https://doi.org/10.1007/s12517-013-1154-4.
Satour, L., Saint Martin, J.P., Belkebir, L., Bessedik, M., 2020. Evolution de la diversité des bivalves messiniens de la bordure méridionale du bassin du Bas Chelif (Algérie Norrd Occidentale). Rev. Paléobiol. 39, 249–263. https://doi.org/10.5281/zenodo.3936169.
Scheffers, S.R., Haviser, J., Browne, T., Scheffers, A., 2009. Tsunamis, hurricanes, the demise of coral reefs and shifts in prehistoric human populations in the Caribbean. Quat. Int. 195, 69–87. https://doi.org/10.1016/j.quaint.2008.07.016.
Scicchitano, G., Monaco, C., Tortorici, L., 2007. Large boulder deposits by tsunami waves along the Ionian coast of south-eastern Sicily (Italy). Mar. Geol. 238, 75–91. https://doi.org/10.1016/j.margeo.2006.12.005.
Seilacher, A., Aigner, T., 1991. Storm deposition at the bed, facies and basin scale: the geologic perspective. In: Einsele, G., Ricken, W., Seilacher, A. (Eds.), Cycles and Events in Stratigraphy. Springer, Berlin, pp. 249–267.
Sessa, J.A., Callapez, P.M., Dinis, P.A., Hendy, A.J., 2013. Paleoenvironmental and paleobiogeographical implications of a Middle Pleistocene mollusc assemblage from the marine terraces of Baía das Pipas. Angola. J. Paleont 87, 1016–1040. https://doi.org/10.1666/12-119.
Shanmugam, G., 2012. Process-sedimentological challenges in distinguishing paleo-tsunami deposits. Nat. Hazards 63, 5–30. https://doi.org/10.1007/s11069-011-9766-z.
Shanmugam, G., 2017. Global case studies of soft-sediment deformation structures (SSDS): Definitions, classifications, advances, origins, and problems. J. Palaeogeogr. 6, 251–320. https://doi.org/10.1016/j.jop.2017.06.004.
Soto, J.I., Déverchère, J., Hudec, M.R., Medaouri, M., Badji, R., Gaullier, V., Leffondré, P., 2022. Crustal structures and salt tectonics on the margins of the western Algerian Basin (Mediterranean Region). Mar. Petrol. Geol. 144, 105820. https://doi.org/10.1016/j.marpetgeo.2022.105820.
Sugawara, D., Goto, K., Jaffe, B.E., 2014. Numerical models of tsunami sediment transport—current understanding and future directions. Mar. Geol. 352, 295–320. https://doi.org/10.1016/j.margeo.2014.02.007.
Sztanó, O., Budai, S., Magyar, I., Csillag, G., Nadrai, J., Fodor, L., 2020. Facies and implications of a coarse-grained lacustrine onshore paleo-tsunamiite: an integrated study of an upper Miocene bouldery cobble gravel. Global Planet. Change 195, 103321. https://doi.org/10.1016/j.gloplacha.2020.103321.
Thomas, G., 1985. Geodynamique d'un bassin intramontagneux, le bassin de Chelif occidental (Algerie), durant le Mio-Plio-Quaternaire. PhD thsesis, Université de Pau et des pays de l'Adour, p. 594. France.
Torres, T., Ortiz, J.E., Puche, O., De La Vega, R., Arribas, Y.I., 2006. Biometría de Strombus bubonius Lamark 1791 del yacimiento de Cerro Largo (Roquetas de Mar, Almería). Geogaceta 40, 167–170.
Torres, T., Ortiz, J.E., Arribas, I., Delgado, A., Julià, R., Martín-Rubí, J.A., 2010. Geochemistry of *Persistrombus latus* Gmelin from the Pleistocene Iberian Mediterranean realm. Lethaia 43, 149–163. https://doi.org/10.1111/j.1502-3931.2009.00180.x.
Torres, T., Ortiz, J.E., Blázquez, A.M., Ruiz Zapata, B., Gil, M.J., Martín, T., Sánchez-Palencia, Y., 2015. The MIS 5 palaeoenvironmental record in the SE Mediterranean coast of the Iberian Peninsula (Río Antas, Almería, Spain). Clim. Past Discuss 11, 3897–3936. https://doi.org/10.5194/cpd-11-3897-2015.
Torres, T., Ortiz, J.E., Mediavilla, R., Sánchez-Palencia, Y., Santisteban, J.I., Vega-Panizo, R., 2022. Assessment of prospective geological hazards in Torrevieja-La Mata coast (western Mediterranean) based on Pleistocene and Holocene events. Nat. Hazards 111, 2721–2748. https://doi.org/10.1007/s11069-021-05155-0.
Vannucci, G., Pondrelli, S., Argnani, A., Morelli, A., Gasperini, P., Boschi, E., 2004. An atlas of Mediterranean seismicity. Ann. Geoph. Suppl. to 47 (1), 247–306.
Wei, W., 1993. Calibration of upper Pliocene-lower Pleistocene nannofossil events with oxygen isotope stratigraphy. Paleoceanography 8, 85–99. https://doi.org/10.1029/92PA02504.
Yesares-García, J., Aguirre, J., 2004. Quantitative taphonomic analysis and taphofacies in lower Pliocene temperate carbonate-siliciclastic mixed platform deposits (Almería Níjar basin, SE Spain). Palaeogeogr. Palaeoclimatol. Palaeoecol. 207, 83–103. https://doi.org/10.1016/j.palaeo.2004.02.002.
Zazo, C., 1999. Interglacial sea levels. Quat. Int. 55, 101–113. https://doi.org/10.1016/S1040-6182(98)00031-7.
Zazo, C., Goy, J.L., Dabrio, C.J., Bardají, T., Hillaire-Marcel, C., Ghaleb, B., González-Delgado, J.A., Soler, V., 2003. Pleistocene raised marine terraces of the Spanish Mediterranean and Atlantic coasts: records of coastal uplift, sea-level highstands and climate changes. Mar. Geol. 194, 103–133. https://doi.org/10.1016/S0025-3227(02)00701-6.
Zazo, C., Goy, J.L., Dabrio, C.J., Lario, J., González-Delgado, J.A., Bardají, T., Hillaire-Marcel, C., Cabero, A., Ghaleb, B., Borja, F., Silva, P.G., Roquero, E., Soler, V., 2013. Retracing the Quaternary history of sea-level changes in the Spanish Mediterranean–Atlantic coasts: geomorphological and sedimentological approach. Geomorphology 196, 36–49. https://doi.org/10.1016/j.geomorph.2012.10.020.